Finite Time Motion Control of a Differential Drive Mobile Robot in a Seed Sowing Line Making Application Using Optimal Adaptive Sliding Mode Controller

Becknam Teshale Chanalo

A Thesis Submitted to the Department of Electrical Power and Control Engineering

School of Electrical Engineering and Computing

Presented in Partial Fulfillment of the Requirement for the Degree of Master's in Control System Engineering

Office of Graduate Studies

Adama Science and Technology University

September, 2024

Adama, Ethiopia

Finite Time Motion Control of a Differential Drive Mobile Robot in a Seed Sowing Line Making Application Using Optimal Adaptive Sliding Mode Controller

Becknam Teshale Chanalo

Major Advisor: Professor SamSun Ma
Co-Advisor: Addisu Safo (MSc)

A Thesis Submitted to the Department of Electrical Power and Control Engineering
School of Electrical Engineering and Computing

Presented in Partial Fulfillment of the Requirement for the Degree of Master's in Control System Engineering

Office of Graduate Studies

Adama Science and Technology University

September, 2024
Adama, Ethiopia

DECLARATION

I hereby declare that this Master Thesis entitled **"Finite Time Motion Control of a Differential Drive Mobile Robot in a Seed Sowing Line Making Application Using Optimal Adaptive Sliding Mode Controller"** is my original work. That is, it has not been submitted for the award of any academic degree, diploma or certificate in any other university. All sources of materials that are used for this thesis have been duly acknowledged through citation.

Becknam Teshale	________________________	________________________
Name of Student	Signature	Date

RECOMMENDATION

We, the advisors of this thesis, hereby certify that we have read the revised version of thesis entitled **"Finite Time Motion Control of a Differential Drive Mobile Robot in a Seed Sowing Line Making Application Using Optimal Adaptive Sliding Mode Controller"** prepared under our guidance by **Becknam Teshale** submitted in partial fulfillment of the requirements for the degree of Mater's of Science in Control System Engineering. Therefore, we recommend the submission of revised version of the thesis to the department following the applicable procedures.

Prof. Sun. Ma	____________________	________________
Major Advisor	Signature	Date
Addisu Safo (MSc.)	____________________	________________
Co-Advisor	Signature	Date

APPROVAL PAGE

We, the advisors of the thesis entitled **"Finite Time Motion Control of a Differential Drive Mobile Robot in a Seed Sowing Line Making Application Using Optimal Adaptive Sliding Mode Controller"** and developed by **Becknam Teshale**, hereby certify that the recommendation and suggestions made by the board of examiners are appropriately incorporated into the final version of the thesis.

Prof. Samsun	______________________________	______________________
Major Advisor	Signature	Date
Addisu Safo (MSc.)	______________________________	______________________
Co-Advisor	Signature	Date

We, the undersigned, members of the Board of Examiners of the thesis by **Becknam Teshale** have read and evaluated the thesis entitled **"Finite Time Motion Control of a Differential Drive Mobile Robot in a Seed Sowing Line Making Application Using Optimal Adaptive Sliding Mode Controller"** and examined the candidate during open defense. This is, therefore, to certify that the thesis is accepted for partial fulfillment of the requirement of the degree of Master of Science in Control System Engineering.

________________________	________________________	________________________
Chairperson	Signature	Date
________________________	________________________	________________________
Internal Examiner	Signature	Date
________________________	________________________	________________________
External Examiner	Signature	Date

Final approval and acceptance of the thesis is contingent upon submission of its final copy to the Office of Postgraduate Studies (OPGS) through the Department Graduate Council (DGC) and School Graduate Committee (SGC).

___________________________	________________________	____________________
Department Head	Signature	Date
___________________________	________________________	____________________
School Dean	Signature	Date
___________________________	________________________	____________________
Office of Postgraduate Studies, Dean	Signature	Date

ACKNOWLEDGMENT

First and foremost, I would like to express my sincere gratitude to Almighty God, the creator of life, the source of all knowledge for granting me the wisdom and perseverance to complete this research paper. I am thankful for the gift of life itself, and for the strength He provided me to conduct this research. His blessings and guidance throughout this journey have been instrumental in making this research a reality.

I would like to express my deepest gratitude to my advisor, **Prof. Samsun Ma**, for his invaluable guidance, constant encouragement, patience, insightful feedback and support throughout this research journey. From the very beginning, **Prof. Samsun Ma** has provided me with the direction and encouragement I needed to navigate the challenges of research.

And I would also like to extend my sincere appreciation to my co-advisor, **Mr. Addisu Safo (MSc)**. His expertise and constructive criticism have been immensely helpful in refining my research and ensuring its clarity. **Mr. Addisu Safo (MSc)** dedication to his students is truly remarkable. He has invested countless hours in helping me to develop my skills and refine my ideas, and his commitment to excellence has inspired me to strive for the highest standards in my work. His passion for his field and his dedication to advancing knowledge are truly inspiring, and I feel honored to have had the opportunity to learn from him.

I am deeply indebted to **Dr. Endalew Ayenew** for his invaluable support and mentorship. His constant encouragement, insightful feedback, and meticulous guidance have been instrumental in shaping this research project. I am grateful for his patience and willingness to share his knowledge, which has significantly improved the quality of this work.

ABSTRACT

This thesis focuses on the control of a differential drive mobile robot, where a dynamic model is derived using the Lagrangian formulation method. The proposed control method utilizes optimal adaptive sliding mode control theory, combining the strengths of sliding mode control and adaptive control laws. To address the challenges posed by the nonlinear model, parameter uncertainties, and external disturbances, a robust adaptive sliding mode control is designed for the speed control system of the mobile robot. Additionally, the use of finite-time integral sliding mode control improves the asymptotic convergence in conventional sliding mode control. Additionally, a potential field function based on gradient descent is employed for obstacle avoidance.The control system consists of two control laws. The kinematic outer loop controller ensures that the posture error and angular error of the mobile robot converge to zero. The second control law utilizes finite-time integral sliding mode control to generate the desired linear and angular velocity, which is compared with the actual velocity. The controller parameters are optimized using particle swarm optimization (PSO) to achieve desired performance in terms of trajectory tracking accuracy, velocity tracking accuracy, and chattering suppression, as measured by the integral time absolute error (ITAE). The stability of the proposed controller is analyzed using the Lyapunov method. The suggested controller demonstrates efficient trajectory tracking, robustness against random external disturbances, and rapid response time with high tracking performance. The effectiveness of the controller is further validated by subjecting the system to various mismatched parameters and random external disturbances. The findings indicate that along the θ axis, the TSMC (ISE) method with model uncertainty resulted in the smallest error of 2.101, while the TSMC (ITAE) method yielded the largest error of 48.87. Similarly, the PSO-ATSMC (ISE) method produced the smallest errors along the X and Y axes, with errors of 2.139 and 2.247, respectively. In contrast, the TSMC (ITAE) method generated the largest errors of 28.27 along the X axis and 42.95 along the Y axis, as shown in Table 5.5. Thus, the PSO-ATSMC demonstrates superior performance in terms of robustness and time-domain measurement metrics, with shorter rise time, settling time, and less overshoot compared to the TSMC without the adaptive law which shown in a Table 5.6.

Keywords:- *Adaptive Control, Lyapunov Method, Sliding Mode Control, Trajectory Tracking, PSO, Mobile Robot, Parameter Uncertainty.*

TABLE OF CONTENTS

LIST OF FIGURES

LIST OF TABLES

LIST OF ABBREVIATION

ATSMC	Adaptive Terminal sliding mode control
DDMR	Differential drive mobile robot
DSMC	Dynamic Sliding Mode Controller
HOSMCO	Higher Order Sliding Mode Control Observer
ILC	Iterative Learning Control
MIT	Massachusetts Institute of Technology
MP	Mobile platform
MPC	Model predictive controller
NMPC	Nonlinear model predictive controllers
PI	Proportional integral
PID	Proportional, Integral, and Derivative Controller
PSO	Particle swarm optimization
SMC	Sliding Mode Control
TWMR	Two-wheeled mobile robots
ZN-PID	Ziegler Nicholas - Proportional Integral Control

CHAPTER ONE

1. INTRODUCTION

1.1. Background

Differential drive mobile robots (DDMRs) are widely used in robotics due to their simplicity, cost-effectiveness, and maneuverability . (Klancar et al., 2017). These robots utilize two independently driven wheels mounted on either side of the robot body, allowing for easy changes in direction by adjusting the relative speeds of the wheels. To ensure stability, DDMRs often incorporate additional castor wheels . (Klancar et al., 2017). Controlling the trajectory of DDMRs has been a challenging task, primarily due to uncertainties and dynamic variations in the system (De Luca et al., 2001). To address these issues, various control techniques such as Sliding Mode Control (SMC) and Adaptive Sliding Mode Control (ASMC) have been developed. These methods aim to mitigate the adverse effects of parameter variations and external disturbances.

An adaptive tracking control technique was proposed to achieve robust performance in the presence of internal and external disturbances (De Luca et al., 2001). The control strategy consists of two main rules. Firstly, an adaptive control rule is implemented to estimate and compensate for parametric uncertainties, enhancing the system's response speed. Secondly, an adaptive robust control rule is employed to handle non-parametric uncertainties in the system. By considering the impact of external disturbances and the varying parameters during robot motion, an adaptive sliding mode controller is designed to ensure that the actual velocity of the DDMR matches the desired velocity. This approach effectively eliminates chattering and effectively handles uncertainties and disturbances throughout the entire robot system (De Luca et al., 2001).

The objective of this research is to navigate a differential drive mobile robot (DDMR) to a desired location while effectively handling disturbances. Sliding mode control (SMC) is a suitable control method for mobile robot applications due to its advantages, including fast response, robustness to system uncertainties, and resilience against external disturbances (Pang et al., 2022), (Mevo et al., 2018).

- The order of the systems can be reduced.
- The systems' behavior is determined by parameters selected by the designer, rather than the process dynamics.
- Once the sliding motion starts, the system's performance is entirely governed by the dynamics of the sliding manifold.

Sliding mode control theory: Sliding mode control is a robust control technique that can be used to control nonlinear systems with uncertainties. Sliding mode control works by driving the system to a sliding surface, which is a surface in the state space of the system. Once the system reaches the sliding surface, it will remain on the sliding surface and track the desired trajectory asymptotically.

Adaptive terminal sliding mode control (ASMC) theory: ASMC is a control technique that combines the advantages of sliding mode control and adaptive control laws. ASMC can achieve the desired performance in finite time without the chattering phenomenon. ASMC works by designing a sliding surface and a control law that drive the system to the sliding surface in finite time. The control law is then adapted in real time to compensate for uncertainties in the system.

Optimal Control theory: is a control theory that deals with the problem of finding the best control input to achieve a desired objective. Optimal control theory can be used to design control scheme that minimize the energy consumption of a system, maximize its speed, or optimize another performance metric.

Motion control in mobile robotics is the process of planning and executing the movement of a mobile robot from one point to another. Motion control systems must take into account the robot's kinematics and dynamics, as well as the environment in which the robot is operating. Kinematics is the study of the motion of objects without regard to the forces that cause the motion. In mobile robotics, kinematics is used to model the relationship between the robot's joint angles and its position and orientation. Dynamics is the study of the forces that cause motion. In mobile robotics, dynamics is used to model the relationship between the robot's inputs (e.g., motor torques) and its outputs (e.g., linear velocity and angular velocity). The environment in which the robot is operating can also have a significant impact on its motion. For example, obstacles in the environment can force the robot to change its trajectory.

DDMRs are characterized by their nonholonomic constraints. Nonholonomic constraints are constraints on the motion of a system that cannot be overcome by choosing the control inputs appropriately. In the case of DDMRs, the nonholonomic constraints are due to the fact that the wheels can only roll and cannot slip. The control of DDMRs is challenging due to their nonholonomic constraints and uncertainties in the system. Traditional motion control schemes, such as PID control, are often not able to achieve the desired performance in terms of trajectory tracking accuracy, velocity tracking accuracy, and chattering suppression. Chattering is a high-frequency oscillation of the control signal that can degrade the performance of the system and even cause instability. Chattering is a common problem with sliding mode control, which is a robust control technique that can be used to control DDMRs. Advantages of actuator modeling are addressed as follows,

Improved accuracy: Actuator modeling can improve the accuracy of the control system by taking into account the dynamics of the actuators. This is important for applications where high precision is required, such as industrial automation and medical robotics.

Increased efficiency: Actuator modeling can increase the efficiency of the control system by reducing the energy consumption of the actuators. This is important for applications where battery life is limited, such as mobile robots and drones.

Improved safety: Actuator modeling can improve the safety of the control system by reducing the risk of actuator saturation. Actuator saturation can cause the robot to become unstable and even crash.

Finally, in this thesis the proposed system ASMC and actuator modeling are promising control techniques for DDMRs and will be implemented in the MATLAB software tool. They offer several advantages over traditional control methods, including

- Robustness to uncertainties,
- Finite-time convergence,
- Chattering suppression,
- Improved accuracy,
- Increased efficiency, and improved safety

1.2. Problem of Statement

The field of mobile robotics has witnessed significant advancements worldwide, enabling a wide range of tasks such as arc welding, painting, environmental inspection, anti-weed spraying, nuclear plant operations, seed planting, and soil nitrogen content measurement, among others. To effectively accomplish these tasks, precise and reliable modeling and control techniques are essential. The ability to achieve fast convergence and high precision control systems is paramount, particularly in the presence of internal and external disturbances. Mobile robots are inherently complex, nonlinear, and multivariable systems with strong interdependencies, making them a highly attractive area of research in recent decades.

However, there are certain limitations that hinder the widespread application of mobile robotics:

- The system can be affected by uncertain nonlinearities, including external disturbances and uncertainties in the model.
- The convergence rate and precision of the control system are crucial factors that need to be addressed.
- Conventional sliding mode control systems often encounter challenges related to asymptotic convergence and chattering phenomena. These issues arise during both the sliding surfaces and reaching phase of the control process.
- In some cases, mobile robot position control is solely based on the kinematic model, neglecting the influence of robot dynamics. However, achieving perfect velocity control without considering the dynamics of mobile robots and various disturbances is practically impossible. Consequently, if there are control faults at the dynamic level, the stability of the kinematic control system may be compromised.

Furthermore, as commonly mentioned in literature, sliding mode control offers several advantages for mobile robotics. It provides fast response, requires minimal information, and exhibits robustness to system uncertainties and external disturbances. This makes it highly suitable for controlling mobile robots. Moreover, external disturbances, such as sudden obstacles or varying friction conditions, can significantly affect the robot's motion, leading to issues like chattering, which further degrade performance. These challenges necessitate the development of an advanced control strategy capable of overcoming these obstacles.

To address these issues, the proposed solution focuses on using an optimal adaptive sliding mode controller (SMC) designed to ensure finite-time convergence with potential field function for obstacle avoidance. This controller is specifically tailored to handle the uncertainties and disturbances associated with DDMRs, enabling accurate trajectory tracking and stable motion control. The optimal adaptive SMC adjusts its parameters in real-time to adapt to changing conditions, thus enhancing the robot's ability to navigate complex environments with precision. By employing this approach, the proposed solution aims to significantly improve the robustness and performance of motion control in DDMRs, ensuring reliable operation even in challenging conditions.

1.3. General Objective

The main objective of this research is to develop an optimal adaptive terminal sliding mode controller, utilizing particle swarm optimization and obstacle avoidance, for the control of a differential drive mobile robot designed for seed sowing line applications.

1.4. Specific Objective

- ✓ Developing the kinematics and dynamic model of differential drive mobile robot using langrage formulation.
- ✓ Design outer loop controller for both angular and posture error to come to zero using outer kinematic controller.
- ✓ Design of a finite time inner loop controller for angular velocity error of each wheel to come to zero under both internal and external disturbances (dynamic speed control system).
- ✓ Tune the parameters of the designed controller using Particle swarm optimization
- ✓ Developing trajectory planner or generator for the obstacle avoidance and detection techniques using a potential field functios.
- ✓ Testing the control algorithms on MATLAB/SIMULINK.

1.5. Scope of The Research

The scope of this research aims to investigate the application of particle swarm optimization (PSO) for gain tuning of an adaptive sliding mode control (ASMC) system, specifically designed for motion control of a mobile robot. The research focuses on addressing the challenges posed by parameter uncertainties in the mobile robot system. The primary objective is to develop an optimized ASMC algorithm that can adaptively adjust its control gains to achieve robust and accurate motion control in the presence of uncertain parameters. The research will involve studying the theoretical foundations of sliding mode control, adaptive control, and PSO algorithms. The emphasis will be on understanding the principles behind ASMC and its ability to handle parameter uncertainties. The PSO algorithm will be explored for optimizing the control gains of the ASMC system to enhance its performance under varying operating conditions.

The system will be subjected to various scenarios, including parameter uncertainties and external disturbances, to evaluate the effectiveness and robustness of the developed control strategy. Performance metrics such as tracking accuracy, convergence rate, and disturbance rejection capability will be analyzed and compared with alternative control methods.

The findings will provide insights into the practical implementation of adaptive control strategies, enabling improved motion control performance in real-world applications with parameter uncertainties.

1.6. Limitations of The Research

While conducting research on particle swarm optimization (PSO) based gain tuning of adaptive sliding mode control (ASMC) for motion control of a mobile robot with parameter uncertainty, several limitations should be acknowledged:

Simplified Model Assumptions: The research may involve making certain simplifying assumptions about the mobile robot's dynamics or the nature of parameter uncertainties. These assumptions may not fully capture the complexities and variations present in real-world scenarios, limiting the generalizability of the findings.

Parameter Uncertainty Modeling: Accurately modeling parameter uncertainties in the mobile robot system can be challenging. The research may rely on simplified or approximate models for parameter uncertainty, which might not fully capture the actual uncertainties encountered in practice. This could affect the performance and robustness of the proposed control approach.

Computational Complexity: Utilizing PSO for gain tuning involves iterative optimization processes, which may have computational complexities. The research should consider the computational requirements and time constraints for implementing the PSO-based gain tuning approach on the mobile robot system, especially in real-time applications.

Limited Experimental Validation: The research may involve experimental validation on a specific mobile robot platform and under specific operating conditions. The findings may be limited to the particular robot and might not account for variations in different robot configurations, environments, or disturbances. Further validation on multiple platforms and in diverse scenarios would enhance the reliability and applicability of the research outcomes.

Practical Implementation Challenges: Implementing the proposed control approach on a physical mobile robot system may introduce practical challenges such as sensor limitations, communication delays, actuator dynamics, and hardware constraints. These factors could influence the real-time performance and overall effectiveness of the control strategy.

1.7. Significance of the Study

A robotic system is critical to the growth of the industry, which is rapidly spreading across Ethiopia. Robots are now utilized in a wide range of industries and applications, including agriculture, aerospace, construction, chemicals, and manufacturing. So, the proposed work has a significant contribution, particularly in the agricultural area, by developing a line of seed sowing that reduces labor force and replaces it with robots by achieving precise, robust controlling trajectory and stable movement of DDMR wheels by improving friction conditions, chattering, uncertainties, disturbances, uneven terrain, variations in the robot's dynamics, and motor characteristics.

1.8. Research Methodology

To achieve the overall objectives of the study, the following methods and techniques will be employed:

Literature Survey: Extensive research will be conducted to review relevant literature and gain a comprehensive understanding of the concepts, theories, and existing approaches related to the thesis topic.

Dynamic Modeling: The dynamic model of the differential drive mobile robot (DDMR) system will be developed. This involves capturing the kinematics and dynamics of the robot and formulating mathematical Equation that describe its behavior.

Controller Design: A finite-time optimal adaptive integral sliding mode control system will be designed for trajectory tracking of the mobile robot. The controller will be specifically designed to handle external disturbances and uncertainties in the system.

Controller Testing: The proposed controller will be rigorously tested under various scenarios and conditions. The controller's performance will be evaluated in terms of its ability to track desired trajectories and its robustness against disturbances and uncertainties.

Performance Comparison: The performance of the designed controller will be compared with alternative control methods or approaches. Time-domain performance metrics such as tracking accuracy, convergence rate, and disturbance rejection capability will be used to assess and compare the controller's performance.

Documentation and Presentation: The results obtained throughout the research process will be documented, analyzed, and summarized. A comprehensive report will be prepared to present the research findings, methodology, and conclusions. Additionally, the findings may be presented in conferences or seminars to share insights with the research community.

The above methodologies will be illustrated in a flowchart, as shown in Figure 1.1, to provide a clear overview of the research process and the interconnections between different stages of the study. Generally, the summarized following Methods have been used for the achievement of this thesis: first, various literature related to the thesis work will be examined. Different concepts are adopted, and a dynamic mode of mobile robot system will be obtained. Then, an optimal adaptive SMC is designed for the trajectory tracking system. Finally, the proposed controller has been tested under different disturbances. Therefore, the above methodologies can be illustrated briefly using the following flowchart, shown in Figure 1.1 below.

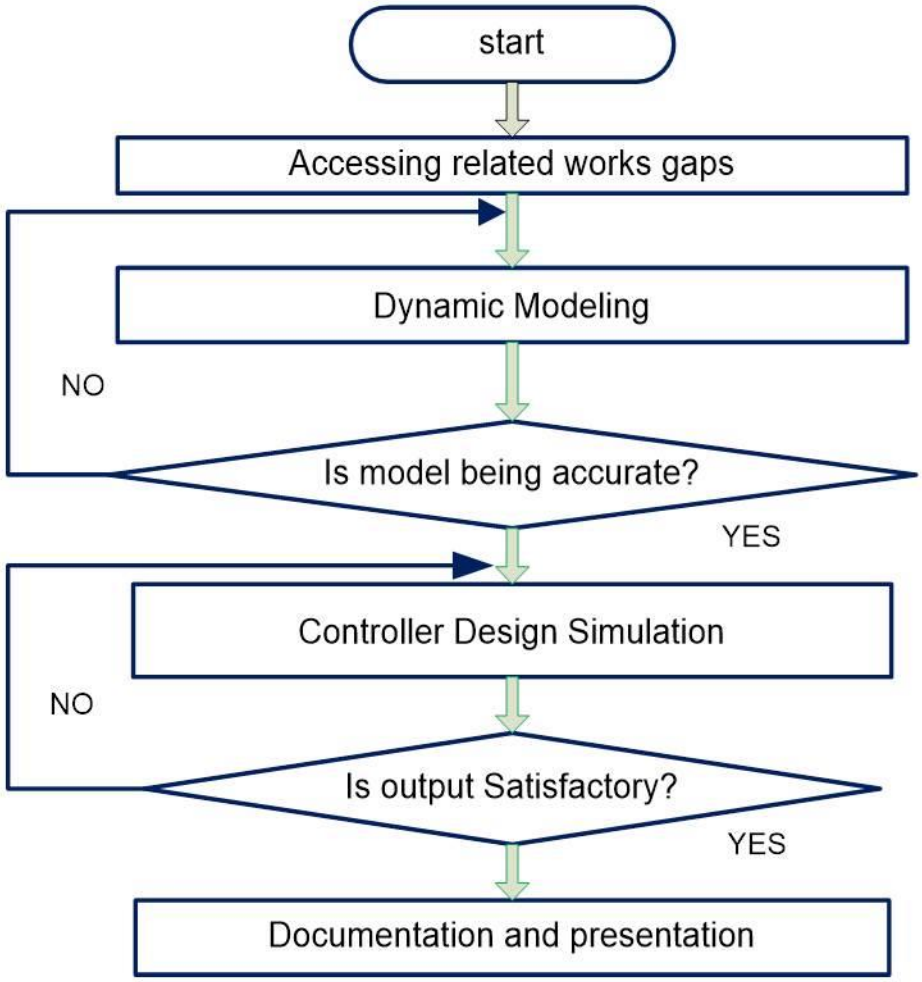

Figure 1. 1: Flowchart of methodology.

1.9. Organization of Thesis Report

The thesis consists of six chapters. The first chapter provides an introduction to the thesis work, highlighting its objectives and significance. The subsequent five chapters are structured as follows:

Chapter 2: Literature Review: This chapter presents an in-depth review of the relevant literature related to the controller for trajectory tracking of differential drive mobile robot systems. The literature review serves to establish a foundation of knowledge and understanding for the thesis.

Chapter 3: Mathematical Modeling: In this chapter, the dynamic model of the mobile robot is derived. The appropriate control and manipulation variables required for controller design are identified based on the mathematical model.

Chapter 4: Controller Design: This chapter focuses on the proposed control scheme, specifically the design of an optimal adaptive sliding mode control system. The design details and considerations for the controller are elaborated upon.

Chapter 5: Results and Discussion: The proposed controller is implemented and tested using Matlab Simulink. This chapter presents the obtained results and provides a comprehensive discussion of the controller's performance and effectiveness in trajectory tracking.

Chapter 6: Conclusion and Future Works: The final chapter concludes the thesis work, summarizing the key findings and contributions. Additionally, future research directions, potential extensions, and identified gaps are discussed to provide avenues for further exploration in the field.

The aforementioned chapter structure ensures a logical progression of the research, from establishing the theoretical foundation to presenting the design, implementation, and evaluation of the proposed controller for trajectory tracking of differential drive mobile robot systems.

CHAPTER TWO

2. LITERATURE REVIEWS

This chapter provides a comprehensive summary of the fundamental concepts and recent literature survey carried out as an integral part of the research presented in this proposal. It encompasses essential established concepts and techniques documented in the literature pertaining to modeling and motion control of differential drive mobile robots (DDMRs).

2.1. Theoretical Background of DDMR

Differential drive mobile robots (DDMRs) are a type of mobile robot that moves using a differential drive system. This mechanism is made up of two independently operated wheels or pairs of wheels, which are usually located on either side of the robot. The robot can perform many sorts of motion, including translations and rotations, by adjusting the rates and directions of rotation of the wheels.(Mathew and Hiremath, 2019)

Differential drive systems move the platform by using two distinct wheels. The two wheels are mounted on either side of the platform and are driven by separate motors. The robot can go forward, backward, and turn by altering the speed of each wheel. The available turning movements vary depending on how the wheels are designed. Figure 2.1 depicts three common differential drive wheel setups. The platform in Figure 2.1a features two powered Conventional wheels (e.g. Segway), but the platform in Figure 2.1b contains an extra Caster wheel in front/back for support. The two platforms, however, may accomplish the identical turning action, including rotating around a vertical axis. The Caster wheel is replaced by a Steering wheel in Figure 2.1c. Given that the steering wheel can be directed quickly enough, this platform has the same mobility as the other two. However, if a steering wheel is used, a kinematic limitation is imposed. This implies that the steering wheel orientation must be adjusted correspondingly (Malu & Majumdar,2014), (Papadopoulos and Misailidis, 2015), (Tagliavini et al., 2022).

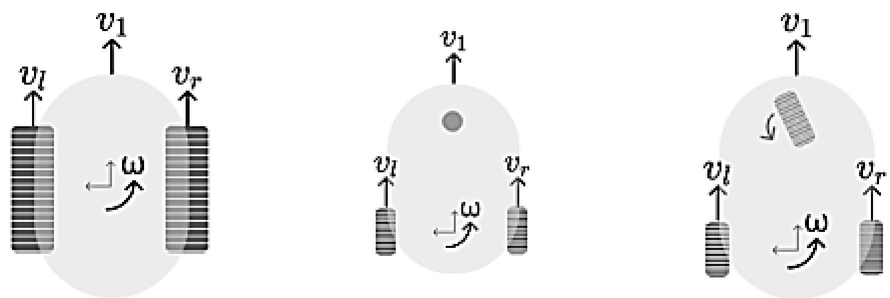

A) Two wheeled b) Caster wheeled c) Car-like

Figure 2. 1: Three types of DDMR

2.1.1. Classification of Differential Drive Mobile Robots (DDMRs)

Differential Drive Mobile Robots are classified in to a various groups based on their structure and on their uses such as: -

Wheeled Differential Drive Robots:

These DDMRs are the robot which is used in this thesis, which have wheels for locomotion, and the differential drive mechanism is implemented using two or more wheels. They are commonly used in indoor environments and can have different wheel configurations, such as two wheels on one side and one wheel on the other side. Wheeled DDMRs are the most common type of DDMR. They are relatively simple to design and build, and they can be used in a variety of environments. Wheeled DDMRs can have different wheel configurations, such as two wheels on one side and one wheel on the other side. This configuration is known as a skid steering configuration. (Torres et al., 2014)

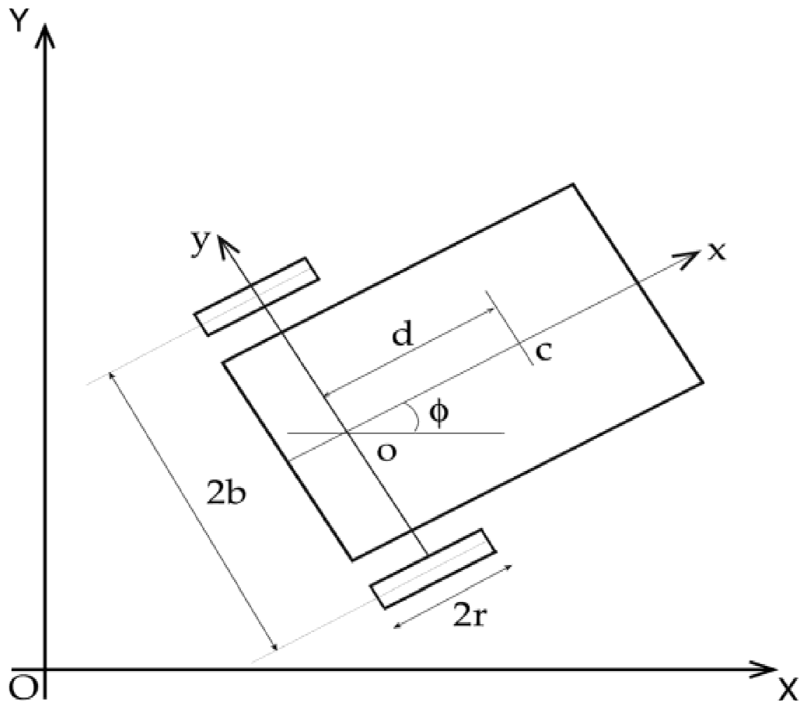

Figure 2. 2: Wheeled Differential Drive Robots (Torres et al., 2014).

Tracked Differential Drive Robots

These DDMRs use tracks or caterpillar treads instead of wheels. The tracks provide better traction and stability, making them suitable for rough or uneven terrains. Tracked DDMRs are often used in outdoor applications, such as agricultural robots or exploration robots. (Ilyas et al., 2013)

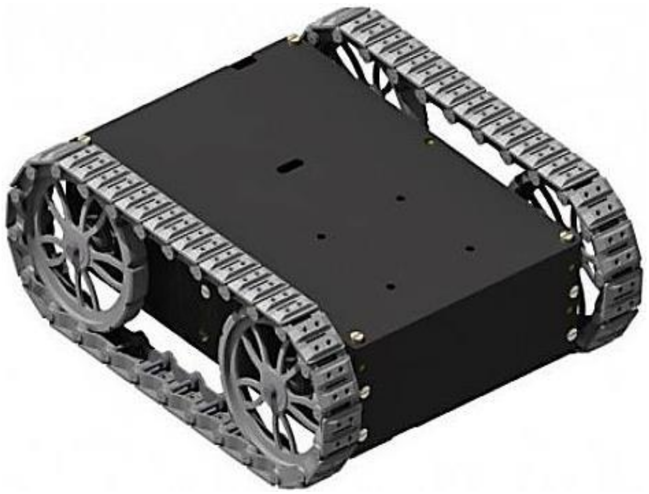

Figure 2. 3: Tracked Differential Drive Robots (Ilyas et al., 2013).

Legged Differential Drive Robots:

This type of DDMR combines the differential drive mechanism with legs for locomotion. The legs enable the robot to traverse various types of terrain, including stairs and rocky surfaces. Legged DDMRs are commonly used in search and rescue missions or for exploring challenging environments. Such as Cassie a bipedal robot, ANYmalia quadrupedal robot, MIT Cheetah 3 is a good example. Legged DDMRs are a relatively new type of robot, but they offer a number of advantages over wheeled and tracked DDMRs. Legged DDMRs are still under development, but they have the potential to revolutionize a wide range of applications, such as search and rescue, exploration, and disaster response. (Xiong et al., 2021)

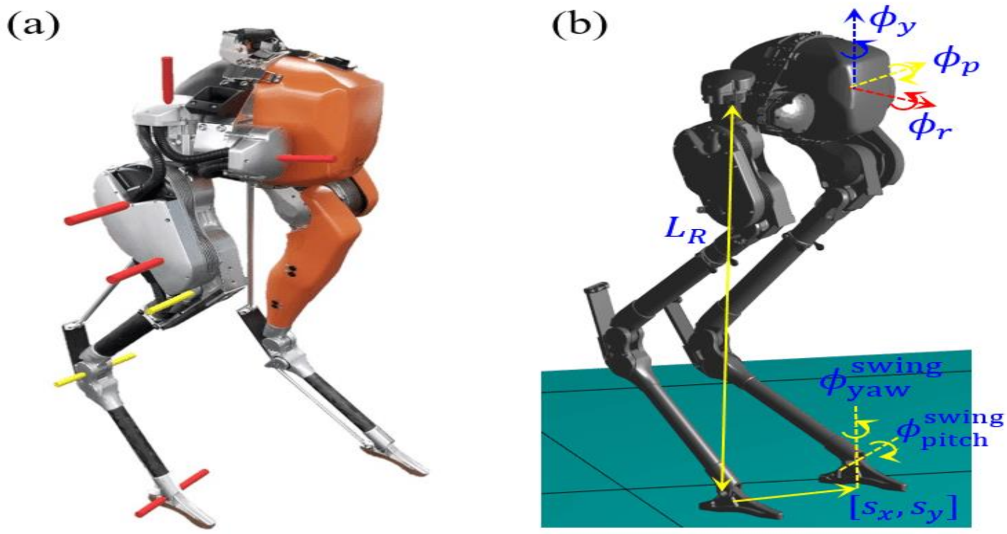

Figure 2. 4: Cassie a bipedal legged DDMR (Xiong et al., 2021).

Hybrid Differential Drive Robots:

These DDMRs incorporate a combination of different locomotion mechanisms, such as wheels, tracks, and legs. The hybrid design allows the robot to adapt to different environments and perform a wide range of tasks. They are often used in advanced robotics research or specialized applications. (Zhao et al., 2021)

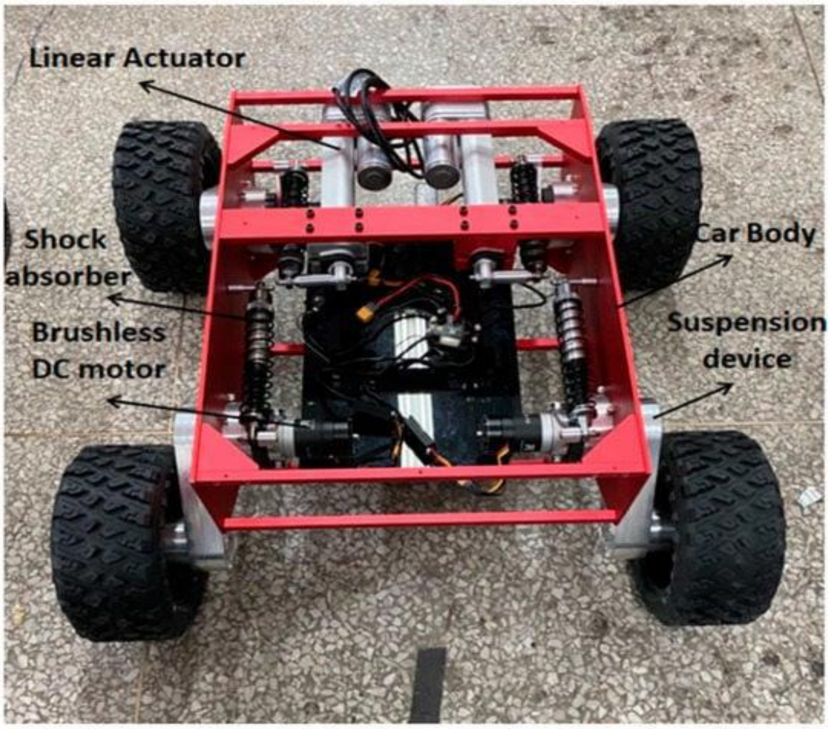

Figure 2. 5: Structure of hybrid DDMR.

2.2. Previous Related Works

The following papers are reviewed to do this thesis proposal concerning with modeling and controlling the proposed system as follow:

Yang Y. et al., (2019) In This study looks into the design and testing of a sliding mode trajectory tracking controller designed particularly for two-wheeled mobile robots (TWMRs). The authors' goal was to create a controller that could perfectly guide a TWMR down a predefined course despite uncertainties and in a limited period of time. But limitation of this tracking is it only based on predefined path and doesn’t consider chattering effect.

Sharma k et al., (2017), The paper investigates trajectory tracking control for non-holonomic mobile robots, a crucial aspect of autonomous systems navigation. It presents an in-depth study of the kinematic Equation that govern non-holonomic robots and delves into the challenges of maintaining a desired trajectory. Furthermore, the research designs nonlinear model predictive controllers (NMPC) employing the derived models to optimize tracking performance. It focuses on minimizing the deviation from set trajectories while addressing input constraints and the decomposition of predicted state variables. The paper limitation is that doesn’t compare others controller such as PID, SMC and etc.

De Luca, a et al., (2001), This research paper provides a comprehensive analysis of various control methods for wheeled mobile robots (WMRs), honing in on the challenges of trajectory tracking and posture stabilization in Nonholonomic systems. The paper exemplifies these principles using a two-wheel differentially-driven mobile robot, Super MARIO, and covers different aspects of WMRs, including their Nonholonomic nature, challenges in point-to-point motion, trajectory following tasks, and control strategies. Moreover, the paper delves into different strategies for posture stabilization. It contrasts smooth and no smooth time-varying feedback controls, highlighting the trade-offs in transient performance and stability when facing mechanical no idealities like backlash. The researchers also advocate for dynamic feedback linearization to circumvent singularities and establish exponential convergence in parking maneuvers.

Keighobadi J et al., (2011), this paper focuses on the design and implementation of a Dynamic Sliding Mode Controller (DSMC) for trajectory tracking control of nonholonomic Wheeled Mobile Robots (WMR). The paper addresses the limitations of conventional linear control theories for trajectory tracking control of WMRs and highlights the advantages of using sliding mode controllers, such as fast response and robustness against perturbations and noises. mentions some existing methods for trajectory tracking control of WMRs, including back-stepping techniques and pole-assignment methods.

The main gap in the paper is that it does not compare the proposed DSMC with other existing sliding mode controllers or other control approaches for trajectory tracking control of WMRs.

Filippo A. et al., (2020), this paper proposes Modeling and Control of a Skid-Steering Mobile Robot for Indoor Trajectory Tracking Applications. The challenge of modeling and control of a nonholonomic Unmanned Ground Vehicle (UGV) for trajectory tracking application is addressed in this thesis. The scientific community has put in a lot of work in the research and development of new modeling approaches, as well as the study of new methodologies targeted at discovering adequate control rules for this type of vehicle. The paper gap is which does not discuss the limitations or potential challenges of implementing the proposed controller in real-world scenarios, such as sensing and actuation limitations or model uncertainties.

In the study conducted by **Kanjanawaniskul K. (2017)** , the focus is on the motion control of a wheeled mobile robot using model predictive control (MPC). The study initially addresses the principles and significant challenges associated with real-time implementations of MPC. Furthermore, an overview of the existing literature on MPC-based motion control is provided. The publications in this field are classified based on three criteria: MPC models, robot kinematic models, and fundamental motion tasks. However, it is important to note that the study does not consider the dynamic interaction between the mobile robot and its kinematics. Additionally, no simulation results are presented regarding the robustness of the controller to external disturbances and nonlinear uncertainties.

Hua Cen et al., (2021), proposed an approach titled "Nonholonomic WMR Trajectory Tracking Control Based on Improved Sliding Mode Variable Structure." The study addresses the issue of inadequate precision in trajectory tracking control for wheeled mobile robots (WMRs) due to their nonholonomic and motion-constrained characteristics. Consequently, the investigation focuses on the nonholonomic WMR tracking system. The study examines the kinematic model and sliding mode control model, and introduces an upgraded variable structure based on sliding mode to control the trajectory tracking of the robot. However, the limitation lies in the fact that the kinematic-level controller is designed without considering the dynamics of the mobile robot, and solely relies on the kinematics of the robot platform.

Al-Dujaili, et al., (2020), the work presented a tracking control scheme for two-link robot manipulators is proposed. The study introduces a super-twisting sliding mode control (STSMC) approach to achieve strong tracking control performance. The stability of the suggested approach is demonstrated using the Lyapunov theorem. Additionally, a social spider optimization technique is employed to adjust the design parameters and enhance the dynamic performance of the robot manipulator controlled by STSMC. Comparative analysis reveals that, in terms of dynamic performance and resilience characteristics, the STSMC technique utilizing social spider optimization outperforms the approach based on particle swarm optimization (PSO). However, it should be noted that a gap in the paper is the absence of an observer or adaptation mechanism to address uncertainties in the system.

Abadi, a et al., (2017), present a paper that introduces an algorithm for generating an ideal trajectory and a controller architecture for a mobile robot. The objective is to develop a performance guidance module for the mobile robot operating in a closed environment. To compute the reference trajectory, an optimization problem is formulated. The combination of differential flatness, B-splines, and the direct collocation method is utilized to transform the constrained optimization problem into a nonlinear programming problem that can be easily solved using a conventional solver. The determined ideal reference trajectory is then incorporated into the kinematic model of the mobile robot. However, it is important to note that the paper does not take into account the motor dynamics, which are not included in the dynamics of the mobile robot. Additionally, the issue of chattering problems is not addressed in the study.

The research conducted by **Sharma R et al., (2016)** focuses on trajectory tracking of a differential drive robot using a mathematical model that encompasses both dynamics and kinematics. The study develops a linear state-space dynamic model by considering the motor dynamics and chassis dynamics of the robot. The basic nonlinear kinematic Equation are linearized to obtain a state-space model that can be sequentially linearized. By combining the dynamic and kinematic models, a single state-space linear model is derived. The reference variables are defined as deviation variables, representing the discrepancies between the actual robot and an ideal robot following a pre-calculated reference trajectory. However, it is important to note that the paper does not address the implementation aspect of the proposed approach, nor does it cover topics such as path planning and obstacle avoidance.

Guo, Y et al., (2019), present a robust finite-time tracking control strategy for wheeled mobile robots in the presence of parametric uncertainties and disturbances. The proposed approach utilizes a nonlinear extended state observer to predict the unknown states and uncertainties, effectively mitigating the impact of lumped uncertainties. Additionally, the appropriate coefficients are adjusted using the pole placement approach. A finite-time sliding mode controller is then designed based on the observed values, ensuring that both the sliding mode variables and tracking errors converge to zero within a finite time. However, it is important to note that the paper does not provide a comparison in different scenarios, such as variations in environmental conditions, obstacle detection, or path planning.

In **Rahul Sharma . et al.,2017**, proposes a thesis that focuses on the dynamic modeling of a differential drive robot and the application of Model Predictive Control (MPC) in both the kinematics and dynamics aspects. The thesis is divided into three sections: kinematic modeling and predictive control, dynamics modeling and control, and Kino Dynamics control. Initially, the nonlinear kinematic Equation are linearized, followed by the derivation of the mathematical model for the dynamics of the mobile robot. Subsequently, the kinematic and dynamics controllers are cascaded, and a comparative study is conducted to evaluate different control strategies. However, it is important to note that the thesis does not consider uncertainties and external disturbances in the control system.

In **E. Fabregas et al., (2020)** present a paper that proposes a closed-loop position control strategy for a mobile robot, enabling it to navigate from its current position to a target point by adjusting its linear and angular velocities. The primary objective of the study is to enhance the response of the robot when it is oriented in a backward direction and to achieve faster reaching of the destination point with a shorter trajectory. This is achieved by modifying an existing control law based on the kinematic model. The stability of the proposed control law is validated using the Lyapunov Criterion. However, it is important to note that this paper solely focuses on the design of the kinematic controller for the mobile robot, disregarding the dynamics of the robot and ignoring the motor dynamics.

In **Doria-Cerezo A. et al., (2019),** present a path-following control algorithm for a differential-drive robot. The paper introduces a novel control formulation that eliminates the need for global position information of the robot. The proposed nonlinear controller, based on the sliding mode control approach, ensures stability in both forward and backward motion. The research focuses on designing a control algorithm for a differential-drive robot that can follow a path, allowing for both forward and backward motion. However, there are certain limitations in the paper. It does not consider variable curvature, particularly when the robot is moving backward. The stability analysis of the entire closed-loop system, including the controller observer, is not addressed.

Benaziza, et.al (2017), proposed "terminal sliding mode control system for trajectory tracking of differential drive mobile robot". Here Only ***steering system (kinematic problem) controller*** was designed but, influence of dynamics of the DDMR was not considered. chattering phenomena due to switching function.

2.3. Summary of Literature Reviews

The above all paper the main gaps which is related to asymptotical convergence in the conventional sliding mode controller, controller design which integrate dynamic of wheeled mobile robot is considered and model uncertainty and robustness to external disturbances. Therefore, using both outer and inner loop controller the effects of dynamic of the mobile robot with model uncertainty solved. Furthermore, using a finite time adaptive integral SMC the asymptotical convergence in the conventional SMC is mitigated as well as the chattering effects also removed for smooth sliding surface.

CHAPTER THREE

3. SYSTEM MODELLING AND METHODOLOGY

3.1. System Description

A differential drive mobile robot is a type of robot with three degrees of freedom, where the motion is controlled by two motors that drive the two front wheels. A third castor wheel is typically present to provide stability and guidance. The robot's position in the world coordinate system is represented by the variables (x, y, θ), with B denoting the midpoint of the robot. Key parameters associated with the robot include the radius of the driving wheels (R), the distance between the center of the robot and its driving wheels (D), and the distance between the robot's center of mass and its rotating center. The model of the differential drive robot, as illustrated in Figure 3.1, is based on the following assumption: The motion of the robot's body is regulated by the two driving wheels located on an axis passing through the geometric center of the robot.

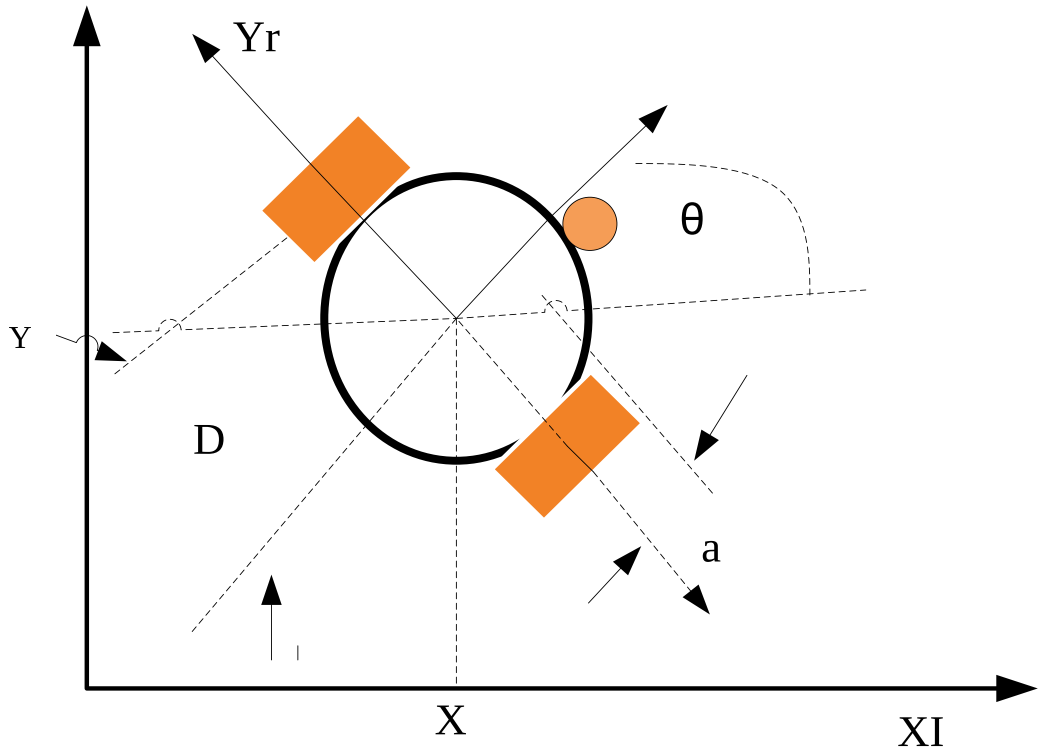

Figure 3. 1:Frame and variable description of DDMR.

3.2. Kinematic and Dynamic Modeling of DDMR

Wheeled mobile robots are classified as non-holonomic machines, meaning they cannot move sideways due to the constraints imposed by the perfect rolling without slipping of their wheels. This unique characteristic restricts their motion to a forward or backward direction and limits their ability to perform lateral movements. In this section, we will delve into this behavior, specifically focusing on the unicycle model (Hatab, 2013).

3.2.1. Kinematic differential drive wheeled mobile robot platform

Kinematic modeling involves the analysis of mechanical system motion without considering the factors that affect the motion (Hatab, 2013). In the case of a differential drive mobile robot (DDMR), the primary objective of kinematic modeling is to describe the robot's velocities based on the velocities of its driving wheels and the geometric attributes of the robot (Hatab, 2013). To accurately represent the position of a wheeled mobile robot (WMR) in its environment, two distinct coordinate systems or frames need to be defined.

In the system of inertial/world coordinate frame, also referred to as the reference frame ({XI, YI}), the position and orientation of the wheeled mobile robot (WMR) are defined. On the other hand, the robot coordinate system is a local frame attached to the WMR, denoted by ({Xr, Yr}), which moves along with the robot as it navigates its environment.

When analyzing a mechanical system, two types of constraints come into play: holonomic constraints and non-holonomic constraints (Hatab, 2013). Holonomic constraints restrict the location or configuration of a system of particles. These constraints can be transformed into constraint integration constants.

In contrast, non-holonomic constraints limit the velocities of particles in a system but not their positions. At least one non-integrable (non-holonomic) constraint is present in such cases.

For a differential drive mobile robot (DDMR), two non-holonomic constraint Equation govern its motion. One such constraint is the absence of lateral slip motion, which means the robot can only move in a forward or backward direction or in the same direction as the plane of rotation of its wheels. This constraint prevents sideways motion, as depicted in Figure 3.2.

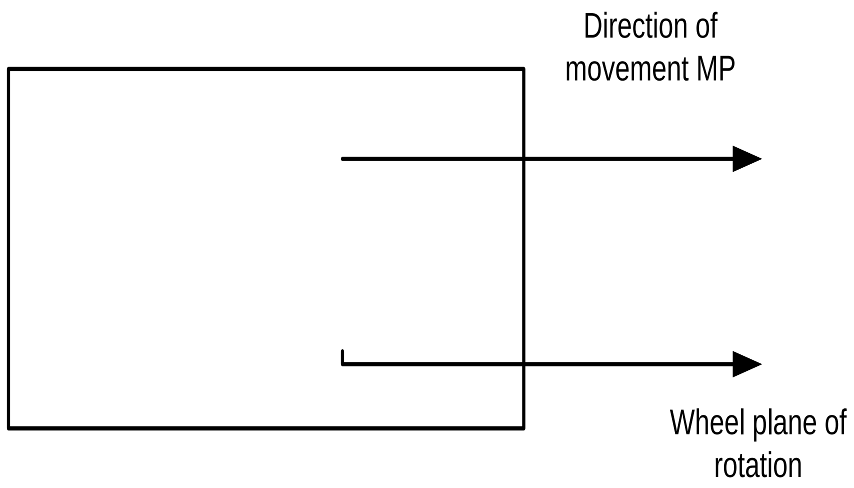

Figure 3. 2:No Lateral slip along vertical axis.

When there is no lateral slip motion the direction of the movement MP is the same as that of wheel's plane of rotation.

$$y_r' = 0 \tag{3.1}$$

The velocity in the inertial frame is calculated using the orthogonal rotation matrix T (θ),

$$cos\theta y_c' - sin\theta x_c' = 0 \tag{3.2}$$

The pure rolling constraint is an important aspect of wheeled mobile robots. It refers to the condition where the wheels of the robot roll without any slipping during motion.

When the robot experiences longitudinal slip, it means that the entire applied torque is effectively transmitted to the ground, causing the wheel to move forward in response to the input torque.

The relationship between the velocities of the wheels and the linear velocities of the robot frame can be expressed as follows:

:

$$v_{pr} = r\phi_r' \tag{3.3}$$

$$v_{pl} = r\phi_l' \tag{3.4}$$

It can be found from Fig 3.1, above that

$$x_i' = cos\theta x_r' - sin\theta y_r' \tag{3.5}$$

$$y_i' = sin\theta x_r' + cos\theta y_r' \tag{3.6}$$

Since the world frame and robot frame share the same z-axis, we can establish the following relationship:

$$\theta_i' = \theta_r' \tag{3.7}$$

By combining Equation (3.5), (3.6), and (3.7), we can conveniently express the relationship as follows

$$\varepsilon_i' = T(\theta)\varepsilon_r' \tag{3.8}$$

Where $$T(\theta) = \begin{pmatrix} cos\theta & -sin\theta & 0 \\ sin\theta & cos\theta & 0 \\ 0 & 0 & 1 \end{pmatrix}$$

The next step is to determine the speed of the robot in its frame by considering the kinematic constraints of the individual wheels. Consequently, we can calculate the forward speed of the wheel, denoted as x', as follows:

$$x_r{}' = r\phi' \tag{3.9}$$

It is crucial to calculate the contribution of each wheel separately, assuming that the other wheels are not activated. In this case, we can consider that the distance traveled by the center point of the robot is exactly half of the distance traveled by each wheel. It is assumed that the non-actuated wheel rotates around its ground contact point.

That is,

$$x_r' = \frac{r\phi_r'}{2} - \frac{r\phi_l'}{2} \tag{3.10}$$

Given the speeds of the right and the left wheels, ϕ_r' *and* ϕ_l', respectively.

The typical wheel constraint dictates that the robot cannot slide, resulting in the y-axis velocity of the robot always being zero (y' = 0). Rotation about the z-axis is accomplished by envisioning the wheels of the robot spinning in opposite directions.

Considering an axle diameter (the distance between the robot's wheels) denoted as D, we can express it as follows:

$$\theta_r' = \frac{r\phi_r'}{2D} - \frac{r\phi_l'}{2D} \tag{3.11}$$

In the inertial frame, the velocities of a differential drive mobile robot (DDMR) can be calculated using the following Equation:

$$\begin{pmatrix} x_i' \\ y_i' \\ \theta_i' \end{pmatrix} = \begin{pmatrix} cos\theta & -sin\theta & 0 \\ sin\theta & cos\theta & 0 \\ 0 & 0 & 1 \end{pmatrix} \begin{pmatrix} \frac{r\phi_r'}{2} + \frac{r\phi_l'}{2} \\ 0 \\ \frac{r\phi_r'}{2D} - \frac{r\phi_l'}{2D} \end{pmatrix} \tag{3.12}$$

The above equation can further expressed as follows

$$\begin{pmatrix} x_i' \\ y_i' \\ \theta_i' \end{pmatrix} = \begin{pmatrix} \frac{rcos\theta}{2} & \frac{rcos\theta}{2} \\ \frac{rsin\theta}{2} & \frac{rsin\theta}{2} \\ \frac{r}{2D} & -\frac{r}{2D} \end{pmatrix} \begin{pmatrix} \phi_r' \\ \phi_l' \end{pmatrix} \tag{3.13}$$

Therefore, the kinematics mobile robot is expressed as

$$\begin{pmatrix} x_i' \\ y_i' \\ \theta_i' \\ \phi_r' \\ \phi_l' \end{pmatrix} = \begin{pmatrix} \frac{rcos\theta}{2} & \frac{rcos\theta}{2} \\ \frac{rsin\theta}{2} & \frac{rsin\theta}{2} \\ \frac{r}{2D} & -\frac{r}{2D} \\ 1 & 0 \\ 0 & 1 \end{pmatrix} \begin{pmatrix} \phi_r' \\ \phi_l' \end{pmatrix} \tag{3.14}$$

If the center of mass of the mobile robot does not coincide with the center of its axle, and the distance from the center of mass to the axle is denoted as a, the kinematic formulation needs to be modified. In this case, we consider the following kinematic Equation (assuming m = 3) at the center of mass (xc, yc) of the robot:

$$\begin{cases} cos\theta y_c' - sin\theta x_c' - a\theta' = 0 \\ cos\theta x_c' + sin\theta y_c' + D\theta' - r\phi_r' = 0 \\ cos\theta x_c' + sin\theta y_c' - D\theta' - r\phi_l' = 0 \end{cases} \tag{3.15}$$

By utilizing the previously defined generalized coordinate vector q = [x_i, y_i, θ_i, ϕr, ϕl]^T for the robot, we can express Equation (3.15) in matrix form as follows;

$$\begin{pmatrix} -sin\theta & cos\theta & -a & 0 & 0 \\ cos\theta & sin\theta & D & -r & 0 \\ cos\theta & sin\theta & -D & 0 & -r \end{pmatrix} \begin{pmatrix} x_i' \\ y_i' \\ \theta_i' \\ \phi_r' \\ \phi_l' \end{pmatrix} = 0 \tag{3.16}$$

Which is equivalent to the kinematic constraint of a non-holonomic system described above, i.e.

$$A^T(q)q' = 0 \tag{3.17}$$

We can select the vector of generalized velocity q = [x_i, y_i, θ_i, ϕr, ϕl]^T for the robot in such a way that it satisfies the constraint equation given by:

$$\begin{pmatrix} x_i' \\ y_i' \\ \theta_i' \\ \phi_r' \\ \phi_l' \end{pmatrix} = \begin{pmatrix} \frac{r(Dcos\theta - asin\theta)}{2D} & \frac{r(Dcos\theta + asin\theta)}{2D} \\ \frac{r(Dsin\theta + acos\theta)}{2D} & \frac{r(Dsin\theta - acos\theta)}{2D} \\ \frac{r}{2D} & -\frac{r}{2D} \\ 1 & 0 \\ 0 & 1 \end{pmatrix} \begin{pmatrix} \phi_r' \\ \phi_l' \end{pmatrix} \tag{3.18}$$

The Equation (3.18) and Equation (3.14) are indeed identical if the center of mass of the entire robot coincides with the center axle, meaning a = 0. In this case, by obtaining the angular speeds of the right and left wheels from wheel encoders, we can determine the position and orientation of the robot by integrating the aforementioned Equation.

3.2.2. Dynamic modeling of DDMR using Lagrange formulation

In the upcoming sections, we will employ the Lagrangian formulation approach to develop the dynamic model of the mobile robot. This approach describes the behavior of a dynamic system in terms of the work and energy stored within the system, rather than focusing on individual forces and moments of its components (Hatab, 2013).

To proceed, we will utilize the schematic diagram of the robot, as depicted in Figure 3.3. The parameters of the robot will be described as follows:

In the formulation of the dynamic model, we define the following parameters for the mobile robot:

R: Radius of the driving wheels.

D*:* Distance between the robot's axle center and each of its driving wheels.

A*:* Distance between a location on the robot's axle center and its center of mass.

mc: Weight of the mobile robot, excluding the motor rotors and the driving wheel*s.*

mw: Combined mass of each driving wheel's motor and its rotor.

Ic*:* Moment of inertia of the mobile robot without driving wheels and the rotors of the motors about a vertical axis, taken at the junction of the robot's Xr-axis and the driving wheel axis.

Iw*:* Rotational inertia of the motor rotor and each driving wheel around the wheel axis.

Iw'*:* Moment of inertia of the rotor and each driving wheel with respect to the wheel diameter.

To begin the formulation, we define the Lagrangain L of the mobile robot as the difference between its kinetic energy T and potential energy U (Hatab, 2013).

$$(q, q') = T(q, q') - U(q) = \frac{1}{2} q'^T B(q) q' - U(q) \tag{3.19}$$

The dynamic Equation of the motion of the mobile robot are generated using Lagrangain formulations, and B(q) is a positive and symmetric definite matrix of the mechanical system as

$$\frac{d}{dt}\left(\frac{\partial L}{\partial q'}\right) - \left(\frac{\partial L}{\partial q}\right) = s(q) + A(q)\lambda \tag{3.20}$$

In the Equation (3.20), s(q) represents an (n x m) matrix that maps the m = n - k external inputs τ to the generalized forces exerted on q. Here, n represents the number of generalized coordinates and k represents the number of constraints. A(q) is the transpose of the (k x n) matrix that represents the kinematic constraints. The vector λ denotes the Lagrangain multipliers associated with the constraints. Similarly, A(q)λ represents the vector of reaction forces at the generalized coordinate level.

At the center of mass of the platform, we compute the components of the speed of the robot as:

$$\theta' = \omega = \frac{r\phi_r'}{2D} - \frac{r\phi_l'}{2D} \tag{3.21}$$

To derive the dynamic model using the Lagrange technique, the first step is to determine the kinetic and potential energy governing the motion of the Differential Drive Mobile Robot (DDMR).

In the case of the DDMR traveling in the XI-YI plane, the potential energy is assumed to be zero since there is no change in height. The total kinetic energy of the DDMR is the sum of the kinetic energies of the robot platform without wheels and the kinetic energies of the wheels and actuators.

The kinetic energy of the robot platform can be expressed as follows:

$$T_c = \frac{1}{2} m_c v_c^2 + \frac{1}{2} I_c \theta'^2 \tag{3.22}$$

The kinetic energy of the right and left wheels can be expressed as follows,

$$T_{wr} = \frac{1}{2} m_w v_{wr}^2 + \frac{1}{2} I_m \theta'^2 + \frac{1}{2} I_w \phi_r'^2 \tag{3.23}$$

$$T_{wl} = \frac{1}{2} m_w v_{wl}^2 + \frac{1}{2} I_m \theta'^2 + \frac{1}{2} I_w \phi_l'^2 \tag{3.24}$$

All velocities will be defined as functions of the generalized coordinates using the general velocity equation in the inertial frame. This equation can be expressed as follows.

$$v_i^2 = x_i^2 + y_i^2 \tag{3.25}$$

In terms of generalized coordinates, the Xi and Yi components of the center of mass and wheels can be calculated as follows:

$$\begin{cases} x_c = x_i + a\cos\theta \\ y_c = y_i + a\sin\theta \\ x_{wr} = x_i + D\sin\theta \\ y_{wr} = y_i + D\cos\theta \\ x_{wl} = x_i - D\sin\theta \\ y_{wl} = y_i + D\cos\theta \end{cases} \tag{3.26}$$

The system's kinetic energy is then conveniently started by combining Equation (3.22), (3.23), (3.24), (3.25) and (3.26) as:

$$T(q, q') = \frac{1}{2} m (x_i^2 + y_i^2) + m_c a \theta' (\cos\theta y_i' - \sin\theta x_i') + \frac{1}{2} I \theta'^2 + \frac{1}{2} I_w (\phi_r'^2 + \phi_l'^2) \tag{3.27}$$

The following new parameters are introduced in this section:

$$m = m_c + 2m_w$$

$$I = 2m_w D^2 + m_c a^2 + 2I_m + I_c$$

Finally, using the Lagrangain formulation provided in, the dynamic Equation of motion for the mobile robot may be written,

$$\frac{d}{dt}\left(\frac{\partial T}{\partial q_i'}\right) - \left(\frac{\partial T}{\partial q_i}\right) = f_i - a_{1i}\lambda_1 - a_{2i}\lambda_2 - a_{3i}\lambda_3 \; for \; i = 1, \dots .5 \tag{3.28}$$

- For q is defined as generalized coordinates,

- f_i represents generalized forces,
- a_{ij} are components of the kinematics constraints
- $A^T(q)$ *and* λ are lagrangain multipliers (Hatab, 2013).

From all of the preceding Equation, we can get the following dynamic model for the mobile robot (3.26) and (3.28) as follows:

$$mx'' - m_c a\theta'^2 cos\theta - m_c a\theta'' sin\theta = -a_{11}\lambda_1 - a_{21}\lambda_2 - a_{31}\lambda_3 \tag{3.29}$$

$$my'' - m_c a\theta'^2 sin\theta - m_c a\theta'' cos\theta = -a_{12}\lambda_1 - a_{22}\lambda_2 - a_{32}\lambda_3 \tag{3.30}$$

$$m_c a(y'' cos\theta - x'' sin\theta) + I\theta'' = -a_{13}\lambda_1 - a_{23}\lambda_2 - a_{33}\lambda_3 \tag{3.31}$$

$$I_w \phi_r'' = \tau_r - a_{14}\lambda_1 - a_{24}\lambda_2 - a_{34}\lambda_3 \tag{3.32}$$

$$I_w \phi_l'' = \tau_l - a_{15}\lambda_1 - a_{25}\lambda_2 - a_{35}\lambda_3 \tag{3.33}$$

The factor a_{ij} are kinematics constraints of the robot defined as $A^T(q)$ i.e.

$$A(q) = \begin{pmatrix} -sin\theta & cos\theta & -a & 0 & 0 \\ cos\theta & sin\theta & D & -r & 0 \\ cos\theta & sin\theta & -D & 0 & -r \end{pmatrix}$$

Therefore, our model reduces to the following Equation:

$$mx'' - m_c a\theta'^2 cos\theta - m_c a\theta'' sin\theta = \lambda_1 sin\theta - (\lambda_2 + \lambda_3) cos\theta \tag{3.34}$$

$$my'' - m_c a\theta'^2 sin\theta - m_c a\theta'' cos\theta = -\lambda_1 cos\theta - (\lambda_2 + \lambda_3) sin\theta \tag{3.35}$$

$$m_c a(y'' cos\theta - x'' sin\theta) + I\theta'' = a\lambda_1 + (\lambda_2 - \lambda_3)D \tag{3.36}$$

$$I_w \phi_r'' = \tau_r + r\lambda_2 \tag{3.37}$$

$$I_w \phi_l'' = \tau_l + r\lambda_3 \tag{3.38}$$

Where, τ_r and τ_l are right and left wheel motor torques.

For the convenience of control system analysis and design, the mobile robot dynamic model in the form of Equation (3.34) to (3.38) can be rewritten in vector form as follows:

$$M(q)q'' + c(q, q') = E(q)\tau - A^T(q)\lambda \tag{3.39}$$

$$M(q) = \begin{pmatrix} m & 0 & -m_c a sin\theta & 0 & 0 \\ 0 & m & m_c a cos\theta & 0 & 0 \\ -m_c a sin\theta & m_c a cos\theta & I & 0 & 0 \\ 0 & 0 & 0 & I_w & 0 \\ 0 & 0 & 0 & 0 & I_w \end{pmatrix}, c(q, q^{\cdot}) = \begin{pmatrix} -m_c a cos\theta \\ -m_c a sin\theta \\ 0 \\ 0 \\ 0 \end{pmatrix},$$

$$E(q) = \begin{pmatrix} 0 & 0 \\ 0 & 0 \\ 0 & 0 \\ 1 & 0 \\ 0 & 1 \end{pmatrix}, \tau = \begin{pmatrix} \tau_r \\ \tau_l \end{pmatrix}, \lambda = \begin{pmatrix} \lambda_1 \\ \lambda_2 \\ \lambda_3 \end{pmatrix} \tag{3.39}$$

Where:

- M(q) represents the inertia matrix of size nxn.

- c (q, qdot) denotes the centripetal and Coriolis forces matrix.
- E(q) is the input transformation matrix.
- τ is the input vector.

3.2. Representation of the model in state space.

To facilitate control system analysis and design, it is essential to express the dynamic and kinematic model Equation of motion of the robot in a form that is easier and more convenient. This can be achieved by employing the concept of state-space realization (Hatab, 2013).

Recalling the two most important system Equation of the differential drive wheeled mobile robot that we developed above, namely Equation (3.14) and (3.39), we can rewrite them in the following form.

$$\begin{pmatrix} x_i' \\ y_i' \\ \theta_i' \\ \phi_r' \\ \phi_l' \end{pmatrix} = \begin{pmatrix} \frac{r(Dcos\theta - asin\theta)}{2D} & \frac{r(Dcos\theta + asin\theta)}{2D} \\ \frac{r(Dsin\theta + acos\theta)}{2D} & \frac{r(Dsin\theta - acos\theta)}{2D} \\ \frac{r}{2D} & -\frac{r}{2D} \\ 1 & 0 \\ 0 & 1 \end{pmatrix} \begin{pmatrix} \phi_r' \\ \phi_l' \end{pmatrix} \tag{3.40}$$

$$M(q)q'' + c(q, q') = E(q)\tau - \quad A^T(q)\lambda \tag{3.41}$$

Here let’s put this differently i.e. in the kinematic model above, letting

$$q = \begin{pmatrix} \frac{r(Dcos\theta - asin\theta)}{2D} & \frac{r(Dcos\theta + asin\theta)}{2D} \\ \frac{r(Dsin\theta + acos\theta)}{2D} & \frac{r(Dsin\theta - acos\theta)}{2D} \\ \frac{r}{2D} & -\frac{r}{2D} \\ 1 & 0 \\ 0 & 1 \end{pmatrix}, and\ \eta = \begin{pmatrix} \phi_r' \\ \phi_l' \end{pmatrix} \tag{3.42}$$

This would give us the same model as above of:

$$q' = s(q)\eta \tag{3.27}$$

The transformation matrix s(q) lies in the null space of the constraint matrix A(q), which can be proven. Consequently, we have the following relationship:

$$s^T(q)A^T(q) = 0 \tag{3.44}$$

The time derivative of equation (3.27) is thus given,

$$q'' = s'(q)\eta + \eta' s(q) \tag{3.45}$$

Equation (3.27) and (3.44) are substituted in the main equation (3.41), we obtain

$$(q)\big(s'(q)\eta + \eta' s(q)\big) + V(q, q')(s(q)\eta) = E(q)\tau - A^T(q)\lambda \tag{3.46}$$

Then, by reshuffling the balance (3.46) and multiplying both sides of $s^T(q)$ by, we get:

$$s^T(q)M(q)\big(s'(q)\eta)\big) + s^T(q)\big(M(q)\eta' s(q)\big) + V(q,q')(s(q)\eta) = s^T(q)E(q)\tau - s^T(q)A^T(q)\lambda \tag{3.47}$$

Where the final term from equation (3.47) is also zero. The new matrices are now being defined:

$$\bar{M}\,(q) = s^T(q)M(q)s(q) \tag{3.48}$$

$$\bar{V}\,(q) = s^T(q)M(q)s'(q) + s^T(q)V(q,q')s(q), and\ \bar{E}\,(q) = s^T(q)E(q) \tag{3.49}$$

The dynamic Equation are simplified to the following form:

$$\bar{M}\,(q)\eta' + \bar{V}\,(q)\eta = \bar{E}\,(q)\tau \tag{3.50}$$

Where $\bar{M}\,(q) = \begin{pmatrix} I_w + \frac{r^2(mD^2+I)}{4D^2} & \frac{r^2(mD^2-I)}{4D^2} \\ \frac{r^2(mD^2-I)}{4D^2} & I_w + \frac{r^2(mD^2+I)}{4D^2} \end{pmatrix}$ (3.51)

$$V(q,q^{\cdot}) = \begin{pmatrix} 0 & \dfrac{r^2 m_c a\theta^{\cdot}}{2D} \\ -\dfrac{r^2 m_c a\theta^{\cdot}}{2D} & 0 \end{pmatrix} = \begin{bmatrix} V_{11} & V_{12} \\ V_{21} & V_{22} \end{bmatrix}, and\ \bar{E}\,(q) = \begin{pmatrix} 1 & 0 \\ 0 & 1 \end{pmatrix}$$

The linear and angular velocities (v, w) of the Differential Drive Mobile Robot (DDMR) can also be utilized to transform the Equation of motion (3.50). It is straightforward to observe how the model Equation (3.50) can be rearranged and compressed into a resulting formula using the kinematic model Equation (3.14).

$$\left(m + \frac{2I_w}{r^2}\right)v' - m_c\, a\omega^2 = \frac{(\tau_r+\tau_l)}{r} \tag{3.52}$$

$$\left(I + \frac{2I_w D^2}{r^2}\right)\omega' - m_c a\omega v = \frac{D(\tau_r-\tau_l)}{r} \tag{3.53}$$

By substituting the expressions of angular and linear velocities from Equation (3.10) and (3.11) into Equation (3.51), we can transform it into an alternative form that is represented by the linear and angular velocities (v, ω) of the Differential Drive Mobile Robot (DDMR).

$$\begin{bmatrix} \left(m + \frac{2I_w}{R^2}\right) & 0 \\ 0 & \left(I + \frac{2L^2}{2R^2} I_w\right) \end{bmatrix} \begin{pmatrix} \dot{v} \\ \dot{\omega} \end{pmatrix} + \begin{bmatrix} 0 & -m_c d\omega \\ m_c d\omega & 0 \end{bmatrix} \begin{pmatrix} v \\ \omega \end{pmatrix} = \begin{bmatrix} \frac{1}{R} & 0 \\ 0 & \frac{L}{R} \end{bmatrix} \begin{pmatrix} u_1 \\ u_2 \end{pmatrix}$$

(3.54)

The simplified form is $\bar{M}\dot{X} + \bar{V}X = \bar{B}u$

$$u = \begin{cases} u_1 = \tau_R + \tau_L \\ u_2 = \tau_R - \tau_L \end{cases} \text{and } X = \begin{pmatrix} v \\ \omega \end{pmatrix}$$

The τ_R represents the torque applied to the right wheel, and τ_L represents the torque applied to the left wheel. Equation (3.54) represents the nonlinear model of the Differential Drive Mobile Robot (DDMR).

To obtain a simplified dynamic model, further simplifications or approximations can be made to Equation (3.54). However, without specific simplifications mentioned, we cannot provide a specific alternative form

$$\begin{bmatrix} m_0 & 0 \\ 0 & I_0 \end{bmatrix} \begin{pmatrix} \dot{v} \\ \dot{\omega} \end{pmatrix} = \begin{bmatrix} \frac{1}{R} & 0 \\ 0 & \frac{L}{R} \end{bmatrix} \begin{pmatrix} u_1 \\ u_2 \end{pmatrix} \tag{3.55}$$

where, m_0 and I_0 are defined as:

$$m_0 = \left(m + \frac{2I_w}{R^2}\right) \text{ and } I_0 = \left(I + \frac{2L^2}{R^2} I_w\right)$$

CHAPTER FOUR

4. CONTROLLER DESIGN

4.1. Trajectory Tracking System Topology

To achieve improved motion and overall control performance, a speed control system should be employed for the Differential Drive Mobile Robot (DDMR). Due to factors such as additional load, surface conditions, and the dynamics of the mobile robot, perfect velocity tracking is often impossible. In such cases, the controller structure is typically split into two stages, as shown in Figure 4.1 (Singh et al., 2020). The inner loop is responsible for controlling the angular velocity of each wheel, taking into account the dynamics of the mobile robot. This inner loop ensures precise control of the individual wheel speeds. On the other hand, the outer loop is a position control system used to control both the translational and rotational positions of the mobile robot. The outer loop determines suitable or desired velocity control inputs that stabilize the kinematic closed-loop control. By employing this two-stage control structure, the outer loop position control system can generate appropriate velocity control inputs to achieve the desired motion and navigate the mobile robot effectively.

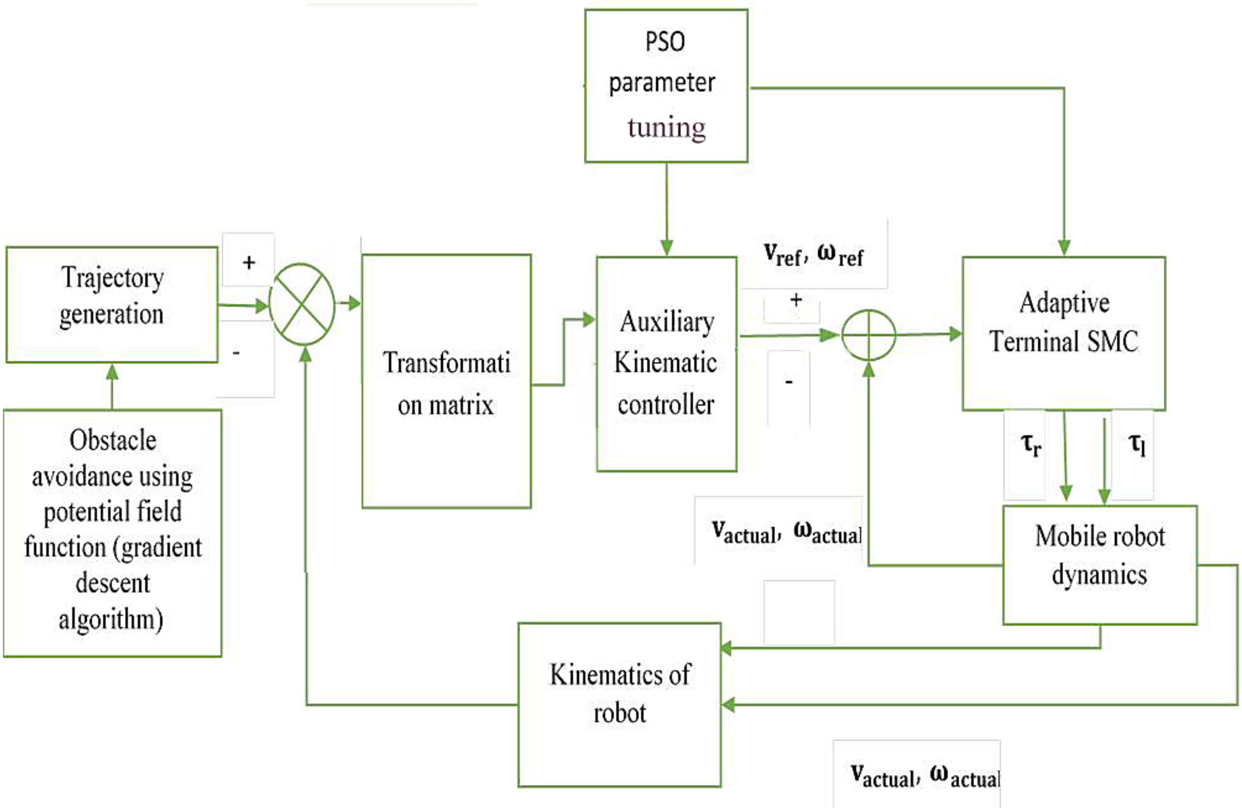

Figure 4. 1:Control system topology.

4.1.1. Algorithm of Kinematic Controller

In order design controller we need two coordinates,

- Reference trajectory denoted as $\mathrm{P_r} = [x_r, y_r, \theta_r]^T$ and
- The actual position and orientation of $P_A = [x_A, y_A, \theta_A]^T$.

Thus, an error posture e_P is defined as follows figure 4.2 below:

$$e_P = \begin{pmatrix} x_e \\ y_e \\ \theta_e \end{pmatrix} = \begin{pmatrix} \cos\ \theta & \sin\ \theta & 0 \\ -\sin\ \theta & \cos\ \theta & 0 \\ 0 & 0 & 1 \end{pmatrix} (P_r - P_A) \tag{4.1}$$

The kinematic controller proposed by (Kanayama et al., 1990) for the Nonholonomic mobile robot is designed to estimate the velocities, both linear and angular, that can ensure asymptotic stability of the system:

$$\begin{pmatrix} v \\ \omega \end{pmatrix} = \begin{pmatrix} v_r \cos\ \theta_e + K_x x_e \\ \omega_r + v_r\left(K_y y_e + K_\theta \sin\ \theta_e\right) \end{pmatrix} \tag{4.2}$$

K_x, K_y and K_θ are positive constants.

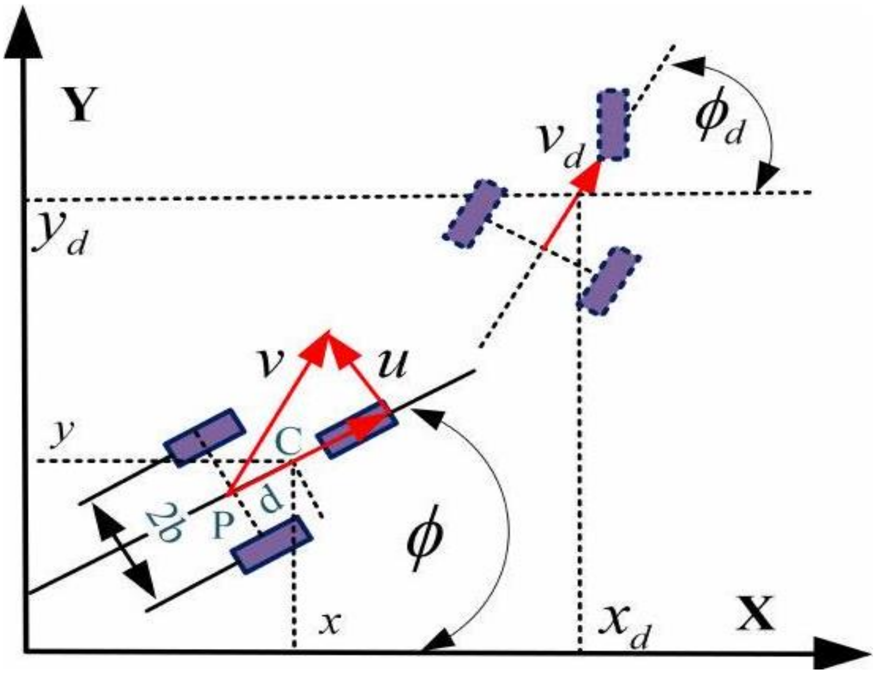

Figure 4. 2: Overview of the differentially driven WMR.

4.1.2. Algorithm of Dynamic Integral Terminal Sliding Mode Controller

To design the dynamic tracking controller for the Nonholonomic mobile robot, the sliding mode control (SMC) method is utilized. In this approach, the SMC is designed for the nominal system, where disturbances are assumed to be zero, the system parameters are known, and the robot model is linear.

To achieve this, an integral terminal sliding surface s is proposed as a mathematical expression, which can be represented as follows (Xu et al., 2019).

$$\mathrm{s} = \mathrm{e} + \beta\left(\int \mathrm{edt}\right)^{\mathrm{p/q}} \tag{4.3}$$

Where the terms p and q are odd numbers which should satisfy the relation $1 < p/q < 2$ and $\beta > 0$.

The sliding surface of the system,

$$\dot{\mathrm{s}} = \dot{\mathrm{e}} + \lambda\left(\frac{\mathrm{p}}{\mathrm{q}}\right) \cdot \mathrm{e} \cdot \left(\int \mathrm{edt}\right)^{(\frac{\mathrm{p}}{\mathrm{q}})-1} \tag{4.4}$$

As presented in (Y. Koubaa et al., 2015), auxiliary velocities tracking error is utilized to determine the input torque.

$$e_x(t) = [e_v, e_w]^T = X(t) - X_d(t) \tag{4.5}$$

$$\dot{e}_x(t) = \dot{X}(t) - \dot{X}_d(t) \tag{4.6}$$

where $X(t)$ is defined in Equation (3.55).

By selecting the sliding surface, this later is defined as:

$$S(t) = \begin{bmatrix} S_1(t) \\ S_2(t) \end{bmatrix} = e_x(t) + \beta\left(\int e_x(t)dt\right)^{p/q} \tag{4.7}$$

$$\dot{S}(t) = \dot{e}_x(t) + \beta\left(\frac{p}{q}\right)e_x(t)\left(\int e_x(t)dt\right)^{(p/q)-1} \tag{4.8}$$

where $\beta > 0$. If the system is on sliding surface $S(t) = 0$ and then $e_c(t = \infty) \to 0$.

$\dot{S}(t) = 0$ is the necessary condition for the state trajectory to stay on the sliding surface.

Eq. (4.8) becomes:

$$\begin{cases} \dot{S}_1(t) = -\dot{v}(t) + \dot{v}_d(t) + \beta\left(\frac{p}{q}\right)e_v(t)\left(\int_0^t e_v(t)dt\right)^{p/q-1} = 0 \\ \dot{S}_2(t) = -\dot{\omega}(t) + \dot{\omega}_d(t) + \beta\left(\frac{p}{q}\right)e_\omega(t)\left(\int_0^t e_\omega(t)dt\right)^{p/q-1} = 0 \end{cases} \tag{4.9}$$

The equivalent control law $u_{eq}(t)$ is:

$$u_{eq}(t) = \begin{cases} u_{eq1}(t) = \gamma\left[\dot{v}_d(t) + \beta\left(\frac{p}{q}\right)e_v(t)\left(\int_0^t e_v(t)dt\right)^{p/q-1}\right] \\ u_{eq2}(t) = \alpha\left[\dot{\omega}_d(t) + \beta\left(\frac{p}{q}\right)e_\omega(t)\left(\int_0^t e_\omega(t)dt\right)^{p/q-1}\right] \end{cases} \tag{4.10}$$

where: $\gamma = m_0R, \alpha = \frac{I_0R}{L}$.

Assuming that all parameters are known, the equivalent control law $\mathrm{u_{eq}}(\mathrm{t})$ can be employed to maintain the state on the sliding surface. However, in real-world applications, the parameters of the robot are often unknown, the robot model is nonlinear, and disturbances are present. In order to address these challenges and ensure the sliding condition is maintained, an adaptive law is proposed to handle the unknown parameters and disturbances.

As a result, the new dynamic equation can be expressed as follows:

$$\begin{cases} \dot{v}(t) = \frac{1}{\gamma} u_1(t) + \Delta_1 \\ \dot{\omega}(t) = \frac{1}{\alpha} u_2(t) + \Delta_2 \end{cases} \tag{4.11}$$

Assuming that Δ1 and Δ2 represent the disturbances, where the uncertainty is bounded and assumed to satisfy |Δ| ≤ D. The new adaptive law is defined as follows:

$$u(t) = u_{eq} + u_w + u_d \tag{4.12}$$

where:

$$u_{eq}(t) = \begin{cases} u_{eq1}(t) = \gamma \left[\dot{v}_d(t) + \beta \left(\frac{p}{q}\right) e_v(t) \left(\int_0^t e_v(t) dt \right)^{\frac{p}{q}-1} \right] \\ u_{eq2}(t) = \alpha \left[\dot{\omega}_d(t) + \beta \left(\frac{p}{q}\right) e_\omega(t) \left(\int_0^t e_\omega(t) dt \right)^{\frac{p}{q}-1} \right] \end{cases}$$

$$u_w(t) = \begin{cases} u_{w1}(t) = K_1 S_1 \\ u_{w2}(t) = K_2 S_2 \end{cases}$$

$$u_d(t) = \begin{cases} u_{d1}(t) = \eta_1 \mathrm{sgn}\,(S_1) \\ u_{d2}(t) = \eta_2 \mathrm{sgn}\,(S_2) \end{cases}$$

u_{eq} is the adaptive compensation, u_w is the feedback item, and u_d is the robustness item. $\hat{\gamma}$ and $\hat{\alpha}$ are respectively estimation of γ and $\alpha. K_1 > 0, K_2 > 0$ and the disturbances are bounded by D, so $|\eta| > D$.

Therefore, the control law can be rewritten as:

$$u(t) = \begin{cases} u_1(t) = \hat{\gamma} \left[\dot{v}_d(t) + \beta \left(\frac{p}{q}\right) e_v(t) \left(\int_0^t e_v(t) dt \right)^{\frac{p}{q}-1} \right] + K_1 S_1 + \eta_1 \mathrm{sgn}\,(S_1) \\ u_2(t) = \hat{\alpha} \left[\dot{\omega}_d(t) + \beta \left(\frac{p}{q}\right) e_v(t) \left(\int_0^t e_v(t) dt \right)^{\frac{p}{q}-1} \right] + K_2 S_2 + \eta_2 \mathrm{sgn}\,(S_2) \end{cases} \tag{4.13}$$

To prove the stability of the kinematic controller, the Lyapunov stability method is employed. Consider a Lyapunov function candidate as follows:

$$L_0 = \frac{1}{2}(x_e^2 + y_e^2) + \frac{1}{K_y}(1 - \cos\ \theta_e) \tag{4.14}$$

Derivative of lyapunov function will be equation 4.14, we get

$$\dot{e}_P = \begin{pmatrix} \dot{x}_e \\ \dot{y}_e \\ \dot{\theta}_e \end{pmatrix} = \begin{pmatrix} \omega(e_p, u_r) y_e - v(e_p, u_r) + v_r \cos\ \theta_e \\ -\omega(e_p, u_r) x_e + v_r \sin\ \theta_e \\ \omega_r - \omega(e_p, u_r) \end{pmatrix} \tag{4.15}$$

Clearly, $L_0 \geq 0, e_P = 0 \Rightarrow L_0 = 0$ and if $e_P \neq 0 \Rightarrow L_0 > 0$ The time derivate of L_0 is $\dot{L}_0 = \dot{x}_e x_e + \dot{y}_e y_e + \frac{1}{\kappa_y}\left(\dot{\theta}_e \sin\ \theta_e\right)$.

We obtain that,

$$\dot{L}_0 = -K_x x_e^2 - \frac{v_r K_\theta \sin^2\ \theta_e}{K_y} \leq 0 \tag{4.16}$$

So that if $v_r \geq 0$ then $\dot{L}_0 \leq 0$. The following proposition show that the uniform asymptotic stability around $e_P = 0$ under the conditions that are $K_x > 0, K_y > 0$ and $K_\theta > 0, v_r$ and ω_r are bounded. v_r and ω_r are continuous.

Considering the challenges of accurately knowing the real values of the robot parameters and disturbances, an adaptive law control (4.13) is proposed. This adaptive law utilizes the estimated parameters, and the simulation is conducted on the nonlinear model of the robot.

In this thesis, we suppose that only m_0 and I_0 are $0 < m_{\min} \leq m_0 \leq m_{\max}$ and $0 < I_{\min} \leq I_0 \leq I_{\max}$.

We select the Lyapunov function as:

$$\begin{cases} L_1 = \frac{1}{2}\gamma S_1^2 + \frac{1}{2a}\tilde{\gamma}^2 \\ L_2 = \frac{1}{2}\alpha S_2^2 + \frac{1}{2b}\tilde{\alpha}^2 \end{cases} a > 0 \text{ and } b > 0 \tag{4.17}$$

Where, $\begin{cases} \tilde{\gamma} = \hat{\gamma} - \gamma \\ \tilde{\alpha} = \hat{\alpha} - \alpha \end{cases}$

Therefore, we get

$$\begin{cases} \dot{L}_1 = \gamma \dot{S}_1 S_1 + \frac{1}{a}\tilde{\gamma}\dot{\hat{\gamma}} \\ \dot{L}_2 = \alpha \dot{S}_2 S_2 + \frac{1}{b}\tilde{\alpha}\dot{\hat{\alpha}} \end{cases} \tag{4.18}$$

In real application, external disturbance affects the system. Eq. (4.18) becomes

$$\begin{cases} \dot{S}_1(t) = -\left[\frac{1}{\gamma}u_1(t) + \Delta_1\right] + \dot{v}_d(t) + \beta\left(\frac{p}{q}\right)e_v(t)\left(\int_0^t\ e_v(t)dt\right)^{p/q-1} = 0 \\ \dot{S}_2(t) = -\left[\frac{1}{\alpha}u_2(t) + \Delta_2\right] + \dot{\omega}_d(t) + \beta\left(\frac{p}{q}\right)e_\omega(t)\left(\int_0^t\ e_\omega(t)dt\right)^{p/q-1} = 0 \end{cases} \tag{4.19}$$

Substituting Equation (4.17) in Equation(4.16), we have:

$$\begin{cases} \dot{L}_1 = \gamma S_1\left[-\dot{v}_d(t) + \left[\frac{1}{\gamma}u_1(t) + \Delta_1\right] + \beta\left(\frac{p}{q}\right)e_v(t)\left(\int_0^t\ e_v(t)dt\right)^{p/q-1}\right] - \frac{1}{a}\tilde{\gamma}\hat{\gamma} \\ \dot{L}_2 = \alpha S_2\left[-\dot{\omega}_d(t) + \left[\frac{1}{\alpha}u_2(t) + \Delta_2\right] + \beta\left(\frac{p}{q}\right)e_\omega(t)\left(\int_0^t\ e_\omega(t)dt\right)^{p/q-1}\right] - \frac{1}{b}\tilde{\alpha}\dot{\hat{\alpha}} \end{cases} \tag{4.20}$$

we have:

$$\begin{cases} \dot{L}_1 = S_1(\gamma - \hat{\gamma})\left(-\dot{v}_d + \beta\left(\frac{p}{q}\right)e_v(t)\left(\int_0^t e_v(t)dt\right)^{p/q-1}\right) - K_1S_1^2 - \eta_1|S_1| - \Delta_1 S_1 - \frac{1}{a}\tilde{\gamma}\dot{\gamma} \\ \dot{L}_2 = S_2(\alpha - \hat{\alpha})\left(-\dot{\omega}_d + \beta\left(\frac{p}{q}\right)e_\omega(t)\left(\int_0^t e_\omega(t)dt\right)^{\frac{p}{q}-1}\right) - K_2S_2^2 - \eta_2|S_2| - \Delta_2 S_2 - \frac{1}{b}\tilde{\alpha}\dot{\hat{\alpha}} \end{cases}$$

(4.21)

We select the adaptive law as:

$$\begin{cases} \dot{\hat{\gamma}} = -aS_1\left(\dot{v}_d + \beta\left(\frac{p}{q}\right)e_v(t)\left(\int_0^t e_v(t)dt\right)^{p/q-1}\right) \\ \dot{\hat{\alpha}} = -bS_2\left(\dot{\omega}_d + \beta\left(\frac{p}{q}\right)e_\omega(t)\left(\int_0^t e_\omega(t)dt\right)^{p/q-1}\right) \end{cases} \quad (4.22)$$

Therefore,

$$\{\dot{L}_1 = -K_1S_1^2 - \eta_1|S_1| - \Delta_1 S_1 < -K_1S_1^2 \leq 0 \quad (4.23)$$

$$\{\dot{L}_2 = -K_2S_2^2 - \eta_2|S_2| - \Delta_2 S_2 < -K_2S_2^2 \leq 0 \quad (4.24)$$

for $|\Delta| \leq D$, asymptotic stability is verified.

To estimate the value of $\dot{\hat{\gamma}}$ and $\dot{\hat{\alpha}}$, we used the discontinuous projection mapping proposed in (J.Liu et al.,2011) .

$$\dot{\hat{\gamma}} = \mathrm{Proj}_{\hat{\gamma}}\ -aS_1\left(\dot{v}_c + \beta\left(\frac{p}{q}\right)e_v(t)\left(\int_0^t e_v(t)dt\right)^{p/q-1}\right)$$

$$\mathrm{Proj}_{\hat{\gamma}}\ (\cdot) = \begin{cases} 0, \text{ if } \hat{\gamma} = \gamma_{\max} \text{ and } \cdot > 0 \\ 0, \text{ if } \hat{\gamma} = \gamma_{\min} \text{ and } \cdot > 0 \\ \cdot\ , \text{ otherwise} \end{cases}$$

and

$$\dot{\hat{\alpha}} = \mathrm{Proj}_{\hat{\alpha}}\ -bS_2\left(\dot{\omega}_c + \beta\left(\frac{p}{q}\right)e_\omega(t)\left(\int_0^t e_\omega(t)dt\right)^{p/q-1}\right)$$

$$\mathrm{Proj}_{\hat{\alpha}}\ (\cdot) = \begin{cases} 0, \text{ if } \hat{\alpha} = \alpha_{\max} \text{ and } \cdot > 0 \\ 0, \text{ if } \hat{\alpha} = \alpha_{\min} \text{ and } \cdot > 0 \\ \cdot\ , \text{ otherwise} \end{cases}$$

4.2. Adaptive Particle Swarm Optimization

The Particle Swarm Optimization (PSO) algorithm is widely used in various fields, including engineering, due to its superior performance compared to other metaheuristic optimization algorithms based on stochastic methods. These algorithms, such as ant colony optimization, follower pollution, grey wolf optimization, and genetic algorithms, exhibit good performance; however, PSO is characterized by its effectiveness and efficiency in finding optimal solutions;

- Superior global value convergence and a high rate of convergence compared to local convergence and
- Excellent precision

Particle swarm optimization is a stochastic method that uses an iterative algorithm to determine the optimal solution (Shi & Eberhart, 1998). At first, it's employed to maximize the continuous space. Generally speaking, the PSO algorithm consists of

- PSO is an optimization algorithm that intelligently selects optimal parameters by iteratively updating the positions of N particles in a D-dimensional search space.
- The algorithm begins with an initialization matrix where N particles are dispersed throughout the search space.
- A fitness function, specific to the problem being solved, is required to evaluate the fitness of each particle's position.
- Each particle, denoted as i, keeps track of its best position P_bi(t+1) and the best solution in its neighborhood g_b(t+1). The neighborhood best position refers to the position of the particle within the swarm that has the smallest fitness value among its nearby particles
- Three rules control the displacement mechanism of each particle.
- Initially, the particle has a tendency to travel in the same direction as its present speed.
- Its second goal is to advance toward its ideal location.
- In the end, it usually moves to the nicest spot that its neighbors have found.

In a group comprising m particles exploring different D-dimensional search spaces, each particle moves at a specific speed. Each particle aims to find the best historical position it has previously encountered, while other particles in the group may also be in their respective best historical positions. The update of a particle's position and speed can be performed using the following formula:

In the three-dimensional position vector of particle i, the PSO algorithm consists of three distinct components:

Recent position of each particle:$\mathrm{x_i} = (\mathrm{x_{i1}}, \mathrm{x_{i2}}, \mathrm{x_{i3}}, \dots . \mathrm{x_{iD}});$

Best position of each particles: $\mathrm{p_{best,i}} = (\mathrm{p_{i1}}, \mathrm{p_{i2}}, \mathrm{p_{i3}}, \dots . \mathrm{p_{iD}})$

The speed of each particles: $\mathrm{v_i} = (\mathrm{v_{i1}}, \mathrm{v_{i2}}, \mathrm{v_{i3}}, \dots . \mathrm{v_{iD}});$

Here,$\mathrm{i} = 1,2 \dots . n.$

In this context, the current position of each particle is represented by a set of coordinates that define its spatial location. At each iteration, the current position is evaluated, and if it yields a better fitness value than the particle's best previous position, an update is made. If the new position is also better than the best position found by any particle within the group, a further update is performed.

It is recorded as follows;

$$g_{best,i} = (g_{best,1}, g_{best,2}\ g_{best,3}, \dots .\ g_{best,D}) \tag{4.25}$$

The following algorithm used for updating,

$$\theta = \theta_{max} - \left(\frac{\theta_{max}-\theta_{min}}{i_{max}}\right) i \tag{4.26}$$

$$\mathrm{v_i}(t) = \theta \mathrm{v_i}(t-1) + \beta_1 * r_1 * \left(p_{best,i} - x_i(t-1)\right) + \beta_2 * r_2 * \left(g_{best} - x_i(t-1)\right)$$

(4.27)

$$\mathrm{x_i}(t) = \mathrm{V_i}(t) + \mathrm{X_i}(t-1) \tag{4.28}$$

Where, usually $\beta_1 = \beta_2 = 2.$]

$$\begin{cases} \mathrm{x_i(t) > x_u, then\ x_i(t) = x_u} \\ \mathrm{x_i(t) < x_l, then\ x_i(t) = x_l} \end{cases} \tag{4.29}$$

The objective function will be evaluated using

$$\mathrm{f_{xi}} = \int_0^{\mathrm{t}} t|e(t)|\mathrm{dt} \tag{4.30}$$

The best position will be obtained as follows;

$$\begin{cases} f_{xi}\ better\ f_{p_{best,i}}, then\ p_{best,i} = x_i \\ f_{p_{best,i}}\ better\ f_{g_{best}}, then\ g_{best} = p_{best,i} \end{cases} \tag{4.31}$$

The Particle Swarm Optimization (PSO) procedure can be outlined as follows:

a) Initialize a population array of particles in the search space, assigning arbitrary locations and velocities in D dimensions.
b) Evaluate the fitness function for each particle to determine its individual optimization objective, aiming to minimize the fitness function in D variables.
c) Compare the fitness value of each particle with its personal best (p_"best"). If the current fitness value is better than the personal best, update p_"best" to the current value and update the corresponding position in D-dimensional space.
d) Update the particle's position and velocity using specific Equation. Additionally, compare the p_"best" values of all particles to find the best fitness value within the swarm, and update the global best position (p_ best) accordingly.

By following these steps, the PSO algorithm iteratively refines the particle positions and velocities, converging towards optimal solutions in the search space.

In order to obtain optimal value of each controller parameters for adaptive SMC sliding mode controller the following flowchart illustrate PSO algorithm.

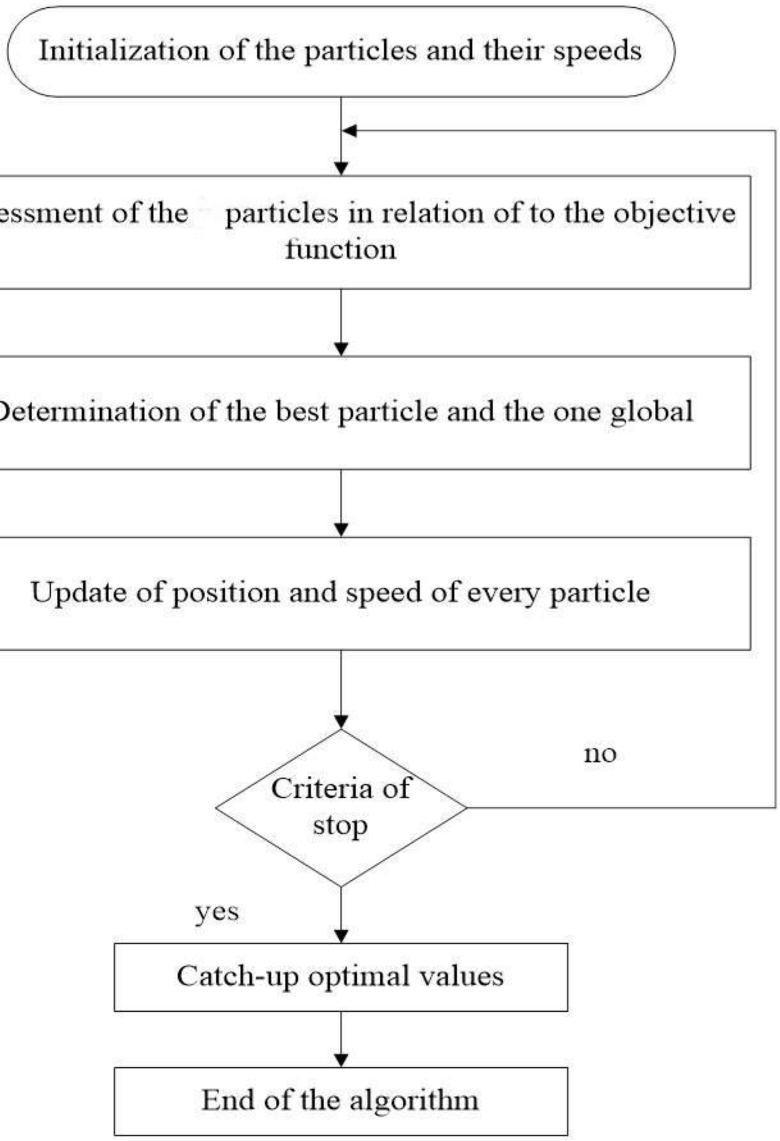

Figure 4. 3: Particle swarm optimization algorithm.

4.3. Obstacle Avoidance with Potential Field Using Gradient Descent Algorithm

Let reference trajectory will be defined as

$$\ddot{x} = u_x \tag{4.32}$$

$$\ddot{y} = u_y \tag{4.33}$$

Where, u_x and u_y are control signal generated using potential field functions.

$$u_x = -\alpha(x - x_d) - \beta\dot{y} + \mu_x \tag{4.34}$$

$$u_y = -\alpha(y - y_d) - \beta\dot{y} + \mu_y \tag{4.35}$$

for $\alpha, \beta > 0$. μ_y, μ_x shown below

Define the position errors as $e_x = x - x_{\mathrm{d}}$ and $e_y = y - y_{\mathrm{d}}$, the coordinates of the object to be avoided as $x_{\mathrm{a}}, y_{\mathrm{a}}$ and a distance function,

$$d_{\mathrm{a}}(\mathrm{x,y}) = \frac{1}{2}(x - x_{\mathrm{d}})^2 + \frac{1}{2}(y - y_{\mathrm{d}})^2 \tag{4.36}$$

We address the obstacle avoidance problem using the following avoidance function defined for $\alpha = \beta = 1$.

$$V_{\mathrm{a}}(\mathrm{x,y}) = \left(\frac{1}{2}\left[\frac{d}{d_{\mathrm{a}}(\mathrm{x,y})} - 1\right]\right)^2 \tag{4.37}$$

Upon taking the partial derivatives of $V_{\mathrm{a}}$with respect to the x and y coordinates, we obtain

$$\frac{\partial V_{\mathrm{a}}}{\partial x} = \left\{ \mathrm{d}\frac{(d_{\mathrm{a}}(\mathrm{x,y}) - \mathrm{d})\ {}^{\partial d_{\mathrm{a}}}/_{\partial x}}{d_a(x,y)^3} \right.$$

$$\text{Where,} {}^{\partial d_{\mathrm{a}}}/_{\partial x} = x - x_{\mathrm{d}}.$$

and

$$\frac{\partial V_{\mathrm{a}}}{\partial y} = \left\{ \mathrm{d}\frac{(d_{\mathrm{a}}(\mathrm{x,y}) - \mathrm{d})\ {}^{\partial d_{\mathrm{a}}}/_{\partial y}}{d_a(x,y)^3} \right.$$

$$\text{Where,} {}^{\partial d_{\mathrm{a}}}/_{\partial y} = y - y_{\mathrm{d}}.$$

Up on the position errors as $e_x = x - x_{\mathrm{d}}$ and $e_y = y - y_{\mathrm{d}}$, r=0, the coordinates of the object to be avoided as $x_{\mathrm{a}}, y_{\mathrm{a}}$, we obtain

$$\begin{cases} \mu_x = -k\dfrac{\partial V_{\mathrm{a}}}{\partial x} & \text{if } d_{\mathrm{a}}(\mathrm{x,y}) \le d \\ 0, & \text{if } d_{\mathrm{a}}(\mathrm{x,y}) < r \end{cases}$$

and

$$\begin{cases} \mu_y = -k\dfrac{\partial V_{\mathrm{a}}}{\partial y} & \text{If } d_{\mathrm{a}}(\mathrm{X,Y}) \le d \\ 0, & \text{If } d_{\mathrm{a}}(\mathrm{X,Y}) < r \end{cases}$$

4.3.1. Lyapunov Stability Analysis Obstacle Avoidance Algorithm

Taking Lyapunov candidate function as:

$$E = \frac{1}{2}(x - x_{\mathrm{d}})^2 + \frac{1}{2}(y - y_{\mathrm{d}})^2 + \frac{1}{2\alpha}(\dot{x})^2 + \frac{1}{2\alpha}(\dot{y})^2 + k\frac{V}{2\alpha} \tag{4.38}$$

Derivative of Eq. (4.32) with respect to time yields:

$$\dot{E} = \dot{x}(x - x_d) + \dot{y}(y - y_d) + \frac{1}{\alpha}\dot{x}\ddot{x} + \frac{1}{\alpha}\dot{y}\ddot{y} + k\nabla V^T \begin{bmatrix} \dot{x} \\ \dot{y} \end{bmatrix} \tag{4.39}$$

$$\dot{E} = \dot{x}(x - x_d) + \dot{y}(y - y_d) + \frac{1}{\alpha}\dot{x}[x - \alpha(x - \ddot{x_d}) - \beta\dot{y} + \mu_x] + \frac{1}{\alpha}\dot{y}\big[-\alpha(y - y_d) - \beta\dot{y} + \mu_y\big] + k\left(\frac{\partial V_{\mathrm{a}}}{\partial x}\dot{x} + \frac{\partial V_{\mathrm{a}}}{\partial y}\dot{y}\right) \tag{4.40}$$

Such that the following holds that,

$$\dot{E} = -\frac{\beta}{\alpha}(\dot{x})^2 - \frac{\beta}{\alpha}(\dot{y})^2 \leq 0 \quad (4.41)$$

From Lassalle's invariance principle, $(\dot{x}, \dot{y}) \to (0,0)$ as $t \to \infty$. Moreover,$(\ddot{x}, \ddot{y}) \to (0,0)$ as $t \to \infty$ from Barbalat's lemma.

Therefore,

$$\ddot{x} = u_x = -\alpha(x - x_d) - \beta\dot{y} + \mu_x = 0 \quad (4.42)$$

$$\ddot{y} = u_y = -\alpha(y - y_d) - \beta\dot{y} + \mu_y = 0 \quad (4.43)$$

From the above equation, we have

$$-\alpha(x - x_d) - \beta\dot{y} - k\frac{\partial V_a}{\partial x} = 0 \quad (4.44)$$

$$-\alpha(y - y_d) - \beta\dot{y} - k\frac{\partial V_a}{\partial y} = 0 \quad (4.45)$$

As it can be seen (x, y) follows (x_d, y_d) when obstacles are not presented.

4.4. High Frequency Oscillation

Chattering, when present in practical implementations, it is a significant factor that can have detrimental effects on the control system. It can lead to damage to actuators and various electronic components, posing a risk to the overall system's functionality and reliability.

In the context of continuous systems, various methods have been explored to address the issue of chattering phenomena, as discussed in reference (Shi & Eberhart, 1998).

A. These methods include:

Techniques for mitigating chattering phenomena:

i. Utilizing the tangent hyperbolic function (tanh(s/ϕ)) along with the implementation of a boundary layer.
ii. Employing continuous approximations of the sign function (sign(s)) instead of the discontinuous sign function.
iii. Applying the saturation function (sat(s,ϕ)) in place of the sign function (sign(s)), along with the use of a boundary layer.
iv. Utilizing algorithms that reduce the domain of the sign function.
v. Implementing the Integral Sliding Mode Control (ISMC) algorithm.
vi. Utilizing the High-Order Sliding Mode Control (HOSMC) algorithm, among others.

B. Continuous approximation functions of the discontinuous sign function:
In order to alleviate chattering, one approach involves substituting the discontinuous sign function with a Continuous Approximation of the Sign Function (CASF). Various functions

have been proposed as potential alternatives for this substitution (Shokouhi & Markazi, 2018)

These methods and continuous approximation functions aim to minimize or eliminate the undesirable chattering phenomenon in control systems

1. To mitigate chattering issues, one approach is to replace the discontinuous sign function with a relay function, also known as a quasi sliding function. By using a relay function, the control system can achieve a quasi sliding mode behavior, which helps reduce chattering. The relay function provides a smooth approximation of the sign function, resulting in improved system performance and reduced oscillations

$$sign(\ s) = \frac{s}{|s|+\delta} \tag{4.46}$$

2. Saturation function instead of sgn function

$$sat(s) = \begin{cases} 1, for\ s > \Delta \\ \frac{s}{\Delta}, abs(s) \le \Delta \\ -1, for\ s < \Delta \end{cases} \tag{4.47}$$

In this approach, a "boundary layer" denoted by Δ is introduced, as depicted in Figure 4.23. The control strategy involves employing switch control outside the boundary layer, while inside the boundary layer, linear feedback control is utilized. This combination of control techniques allows for a smooth transition between different control modes, effectively addressing the chattering phenomenon and improving the overall system performance.

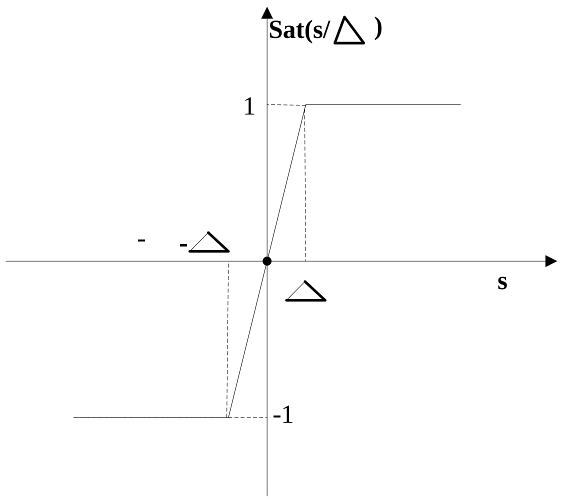

Figure 4. 4: Bounder functions.

3. To mitigate the undesirable high-frequency oscillation behavior caused by the nonlinear discontinuous term in the system response, this research proposes replacing the nonlinear signum function with an inverse tangent function. The inverse tangent function is a continuous function, offering a smoother and more continuous

representation compared to the signum function. By substituting the signum function with the inverse tangent function, the system response can exhibit improved behavior with reduced oscillations;

$$sign(s) = tan^{-1}(s * \Delta) \tag{4.48}$$

Where, $\Delta > 1$

CHAPTER FIVE

5. SIMULATION RESULT AND DISCUSSION

5.1. Open Loop Analysis and Results of Simulation

To mimic robotic systems and carry out simulations for this project, we utilized MATLAB and MATLAB/Simulink, which are powerful software tools widely employed in robotics research. The proposed Lagrange dynamic modeling approach for mobile robot dynamics is implemented in MATLAB/Simulink to evaluate the dynamic simulation and assess the system in this part.

5.2. Simulation block diagram for the entire mobile robot dynamic system

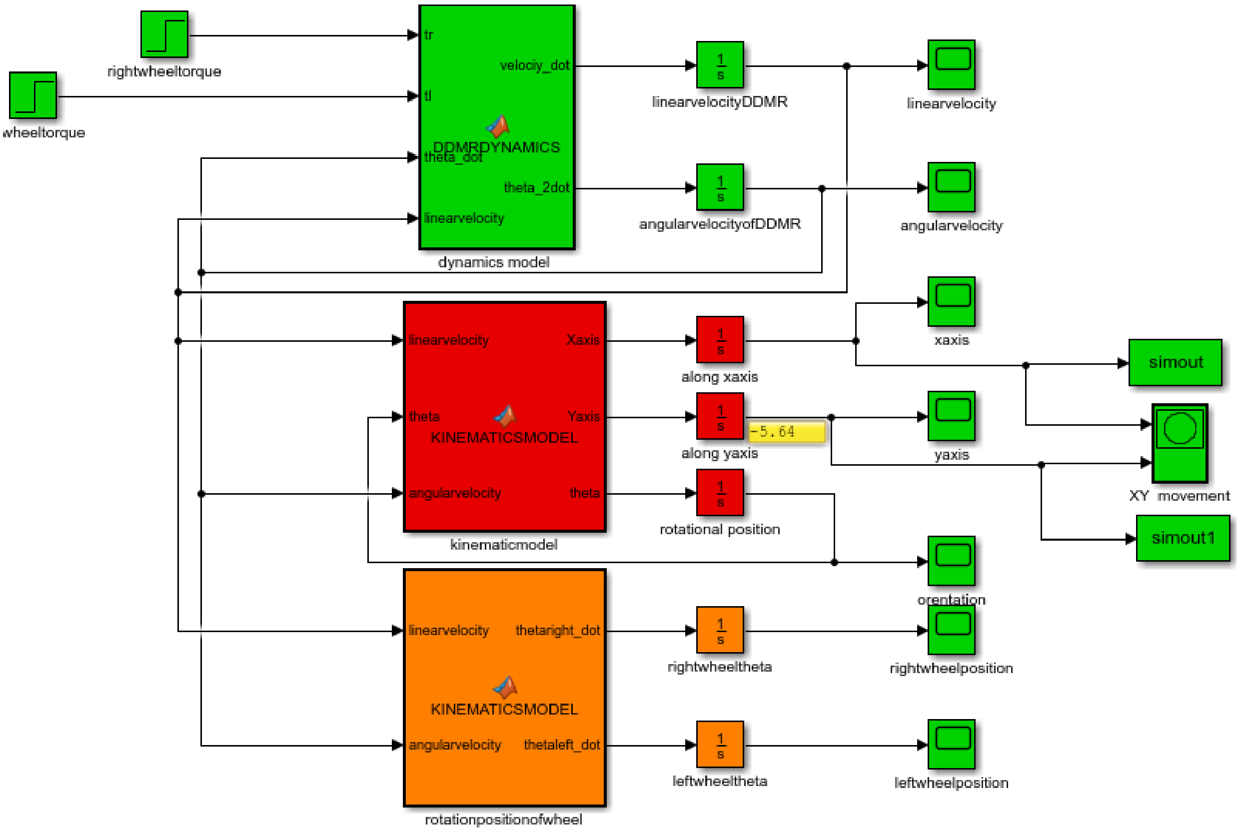

Figure 5.1: Simulink block diagram to simulate the mechanical element of the robot model.

The block diagram provided above represents the mechanical model of a differential drive mobile robot. By applying different torques to the mechanical model as the output of the right and left wheel actuators, we can assess the robot's motion in response to these varying torques.

To simulate the robot's mechanical model, Equation (3.51) to (3.52) for the dynamic model and equation (3.13) for the kinematic model are implemented in MATLAB/Simulink, as illustrated in Figure 5.1.

Once the model is built in MATLAB/Simulink, it is necessary to define the robot settings and generate various tests to ensure the functionality of the model. Table 5.1 presents the robot parameters used to simulate the model (A. Sharma & Panwar, 2016).

Table 5. 1:Numerical parameter values of DDMR used for simulation.

Parameter	Value and unit
m_c	0.5 kg
m_w	17 kg
D	0.05 m
L	0.24 m
R	0.095 m
I_c	$0.537\ \mathrm{kg}\cdot\mathrm{m}^2$
I_m	$0.0011\ \mathrm{kg}\cdot\mathrm{m}^2$
I_w	$0.0023\ \mathrm{kg.m}^2$

For the adaptive model parameter estimation, $17.51\ \mathrm{kg} \leq m_0 \leq 37.51\ \mathrm{kg}$; $0.57\ \mathrm{kg}\cdot\mathrm{m}^2 \leq I_0 \leq 4.57\ \mathrm{kg}\cdot\mathrm{m}^2$; $v_r = 1\mathrm{m/s}$; $\omega_r = 0\mathrm{rd.s}^{-1}$.

In this section, we analyze the impact of inputs on the output state by calculating the inputs for each wheel, specifically the right and left wheels of a mobile robot, using torque inputs. By adjusting the torque inputs, we can observe the corresponding changes in the output state of the robot. This analysis helps us understand how the inputs affect the motion and behavior of the mobile robot.

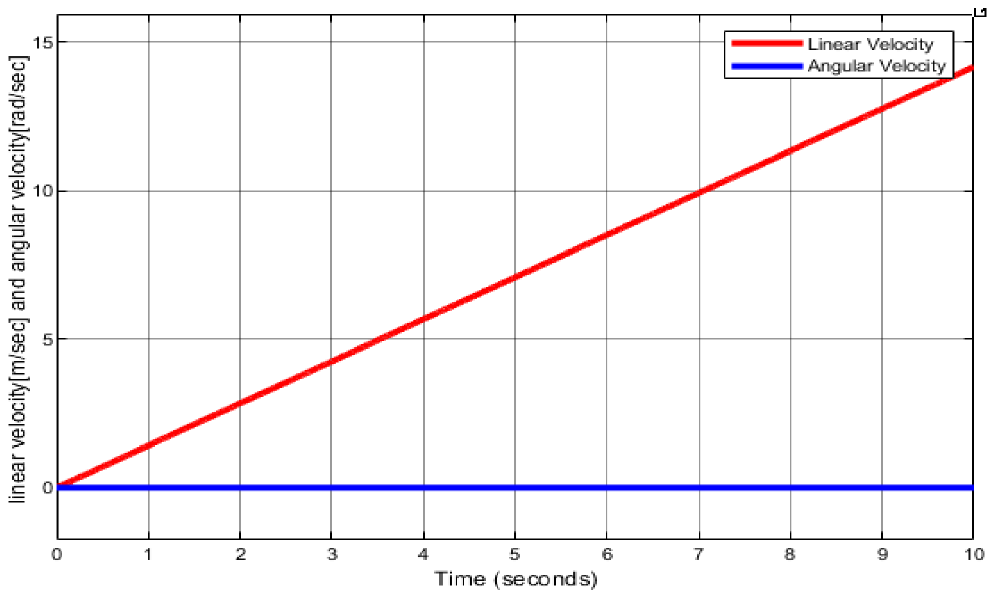

Figure 5.2: Linear and angular velocity

From Figure 5.2, it is evident that the differential drive mobile robot moves in the XY plane with a combination of linear and angular velocities. When both wheels are activated with equal torques of 0.78 Nm and the rotational position of the DDMR is zero, the angular velocity along the XY plane will indeed be zero. Consequently, the robot will only accelerate in the direction of the X-axis, maintaining a straight trajectory without any rotational motion.

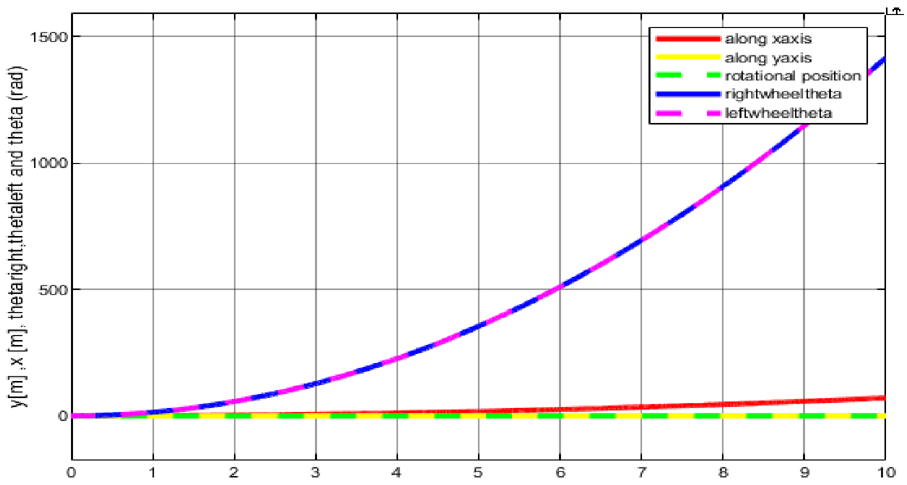

Figure 5.3: X axis, Y axis, rotational position, rotational position (left wheel theta) and rotational position (right wheel theta) under 0.78Nm torque input.

Based on Figure 5.3, it can be observed that the mobile robot only moves along the X-axis, while its translational position along the Y-axis remains at zero. This indicates that the robot is moving forward solely in the X-axis direction, without any lateral motion.

Furthermore, from Figure 5.4, it is evident that the application of a constant torque of 0.78 Nm causes the mobile robot to move forward along the XY plane, as depicted. In this particular scenario, the robot covers a distance of approximately 72 meters in 10 seconds, resulting in an average velocity of 7.2 meters per second.

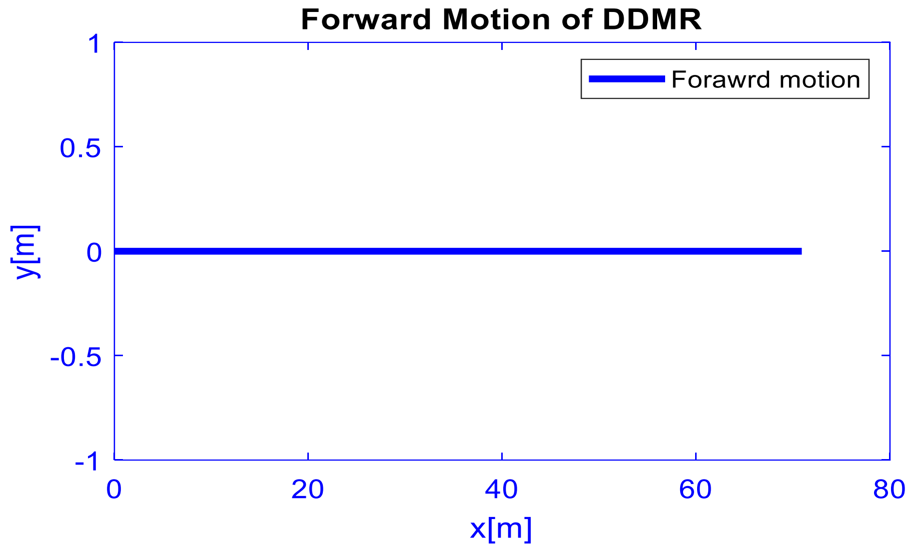

Figure 5. 4: Forward motion by applying positive torques of 0.78Nm to each wheel

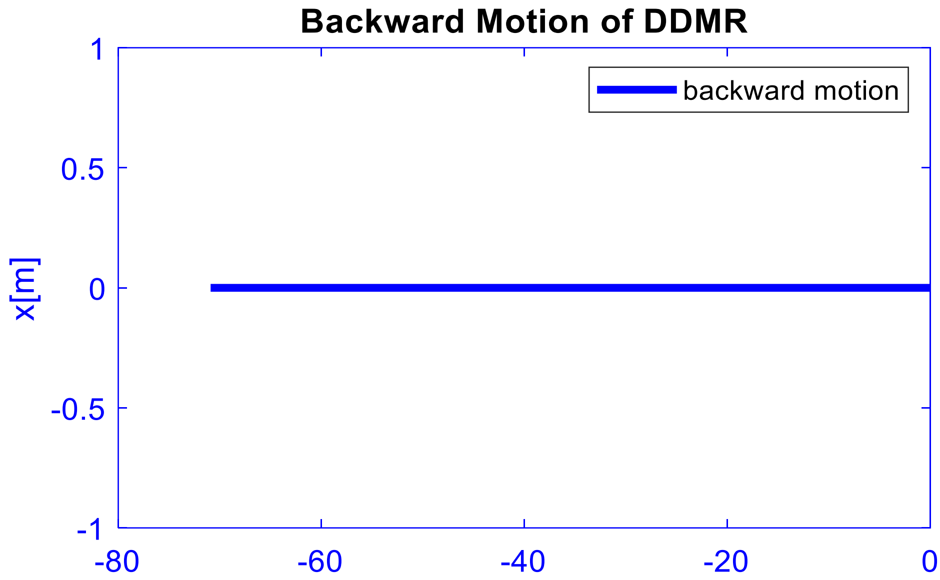

Figure 5.5: backward motion by applying negative torques of -0.78Nm to each wheel

As depicted in Figure 5.5, the robot covers the same distance of 72 meters when moving in reverse as it does when moving forward. The distance traveled depends on the magnitude of the negative torque applied to each of the DDMR wheels and the corresponding position of each wheel's rotation. By controlling the negative torques appropriately, the robot is able to achieve the desired reverse motion and cover the same distance as it did while moving forward.

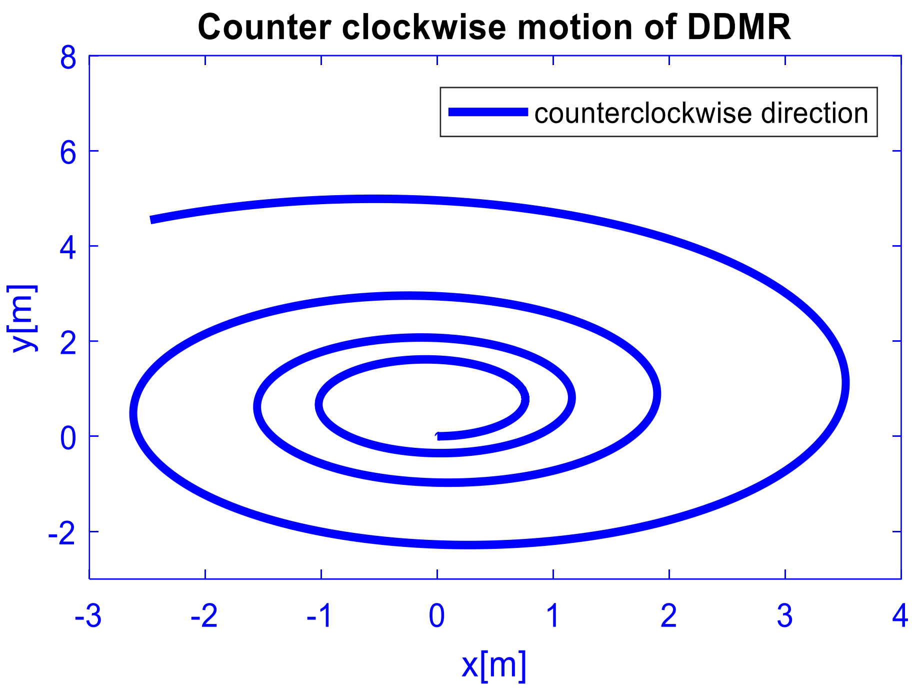

Figure 5.6: Counter Clockwise Motion

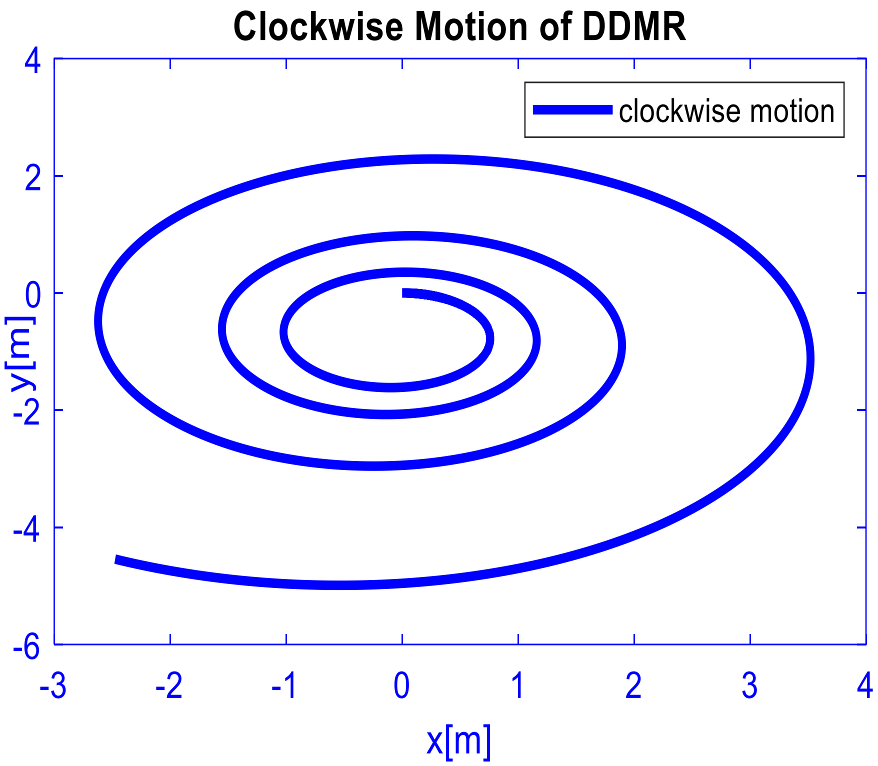

Figure 5.7: Clockwise Motion of DDMR

In Figures 5.6 and 5.7, we observe the motion of a mobile robot when only one wheel is actuated by a motor. From the graphs, it is evident that the robot moves in opposite directions depending on which wheel is being driven.

When only the left wheel is moved, the robot moves in one direction, while moving only the right wheel causes the robot to move in the opposite direction. This demonstrates the differential drive mechanism of the mobile robot, where asymmetric wheel velocities lead to differential motion and enable the robot to maneuver and change its direction of travel.

5.3. Simulation Result of the Overall Tracking Control for Mobile Robot

In this part, MATLAB/Simulink is utilized to implement the suggested controller approach for the mobile robot, enabling the simulation of system stability and validation. The MATLAB programming environment is chosen to simulate the proposed control and visualize the motion of the mobile robot. In this section, through computer simulations performed in MATLAB/Simulink, we evaluate the capability of the proposed controller to stabilize the mobile robot while considering different time-parameterized reference signals for trajectory tracking in the control system. This allows us to assess the controller's performance in accurately tracking desired trajectories and maintaining stability in the robot's motion.

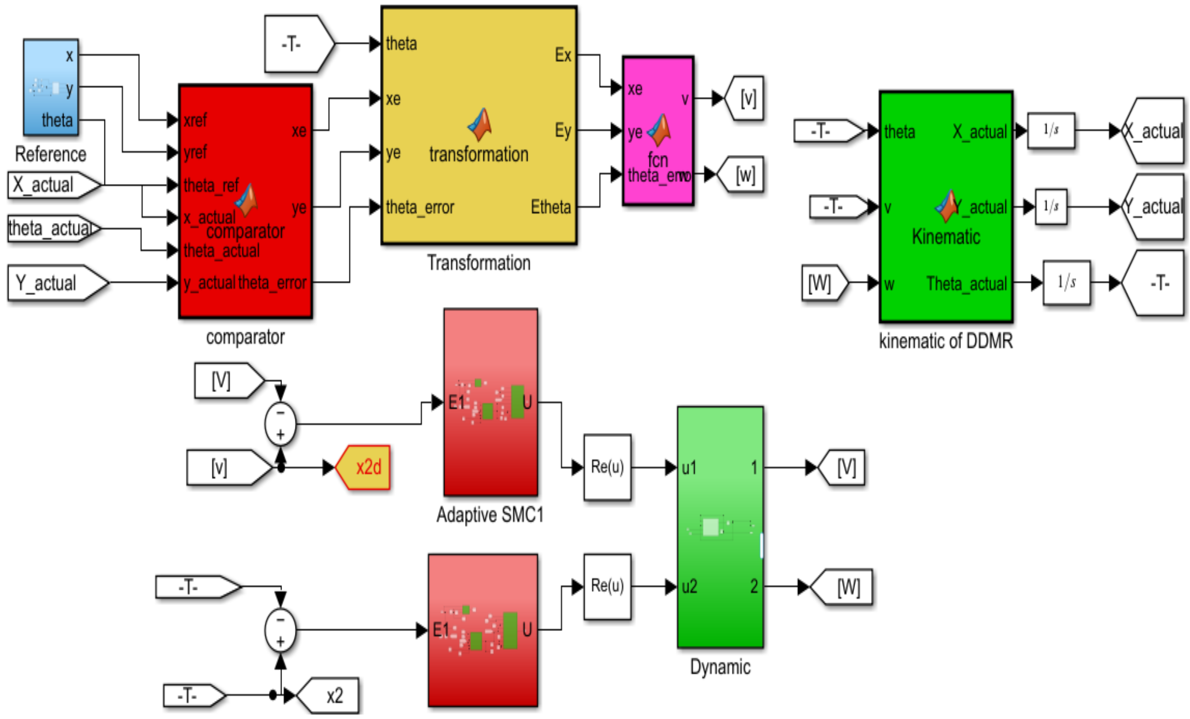

Figure 5. 8: Simulink block diagram.

As depicted in the Simulink block diagram in Figure 5.8, the main blocks of the system are as follows:

1. Kinematic level controller (outer loop) for the differential drive mobile robot (DDMR).
2. Forward and inverse kinematics blocks for the DDMR, which handle the translation and rotation calculations.

3. Dynamic controller (inner loop) with the dynamic model of the DDMR for controlling the robot's motion.

In this section, we have delved into the proposed control system in detail, focusing on its tracking performance by providing desired trajectories for the robot's states. The following figures showcase the performance of the optimal adaptive sliding mode control (SMC) controller for each individual state simultaneously, demonstrating the controller's effectiveness in achieving desired tracking performance.

In this thesis, the following reference trajectories have been selected for simulation purposes in order to seed sowing line making ability of mobile robot under presence of static obstacles:

Table 5. 2: Reference Trajectory for seed sowing line making robot.

Reference trajectory controller parameter	Unit
$v_r = 1$	m/sec
$\omega_r = 0$	rad/sec
$xd(t) = t$	Meter
$yd(t) = 3$	Meter

Both the controller settings for the dynamic controller (inner controller) and the controller parameters for the design of the kinematic level (outer controller) for the mobile robot are is chosen using particle swarm techniques.

Table 5. 3:Controller parameters using PSO.

Parameters of proposed controller for DDMR	
Inner controller	Outer controller
$k_x = 1$ $k_y = 1.5$ $k_\theta = 2.2$	$K_1 = 1, K_2 = 150, \eta_1 = 2$, and $\gamma_1 = 0.1$ P=5 and q=3
	$K_1 = 1, K_2 = 150, \eta_2 = 2$, and $\gamma_2 = 0.1$

Table 5. 4: Specification of Parameters PSO.

Particle swarm particle parameters
$\theta_{max} = 0.9, \theta_{min} = 0.1, \beta_1 = \beta_2 = 2$

Number of particles =20
Number of iterations=30
$x_{u1} = 2, x_{l1} = 0.1$
$x_{u2} = 1000, x_{l2} = 0.1$
$v_0 = 0$
Initial position selected random between upper and low

Demonstration of the control system is evaluated for various initial conditions, where the starting position of the mobile is as follows. The simulation time for trajectory tracking is 25 seconds if the mobile robot starts from its original position of (-1m, 0 m, 0 rad/sec), and the suggested control can implement the tracking system whenever it is desired. The accuracy and effectiveness of both inner and outer loop controllers against model uncertainty was tested using different performance index measurements such as integral absolute error (IAE), integral time absolute error (ITAE), integral time square error (ITSE), and integral time absolute error (ITAE) as presented in Table 5.5 below.

Table 5. 5: Controller Performance Comparison.

Error along	PSO-ATSMC				TSMC			
	ISE	ITSE	IAE	ITAE	ISE	ITSE	IAE	ITAE
X axis	2.139	7.751	4.609	24.91	3.123	10.22	5.418	28.27
Y axis	2.247	7.579	4.537	21.34	1.94	11.9	5.079	42.95
Theta	2.111	9.985	4.82	34.9	2.101	13.79	5.33	48.87

The analysis indicates that with model uncertainty, the smallest error of 2.101 along the θ axis was obtained using TSMC (ISE), while the largest error of 48.87 was recorded along the θ axis using TSMC (ITAE). Additionally, the PSO-ATSMC (ISE) method achieved the lowest errors of 2.139 and 2.247 along the X and Y axes, respectively. In contrast, TSMC (ITAE) resulted in the highest errors of 28.27 and 42.95 along the X and Y axes, as detailed in Table 5.5. Consequently, the PSO-ATSMC method demonstrates superior performance in terms of robustness and time-domain metrics, featuring reduced rise time, settling time, and overshoot compared to the conventional TSMC without the adaptive component.

5.4. Performance of Adaptive Sliding Mode Control Under mismatching uncertainty

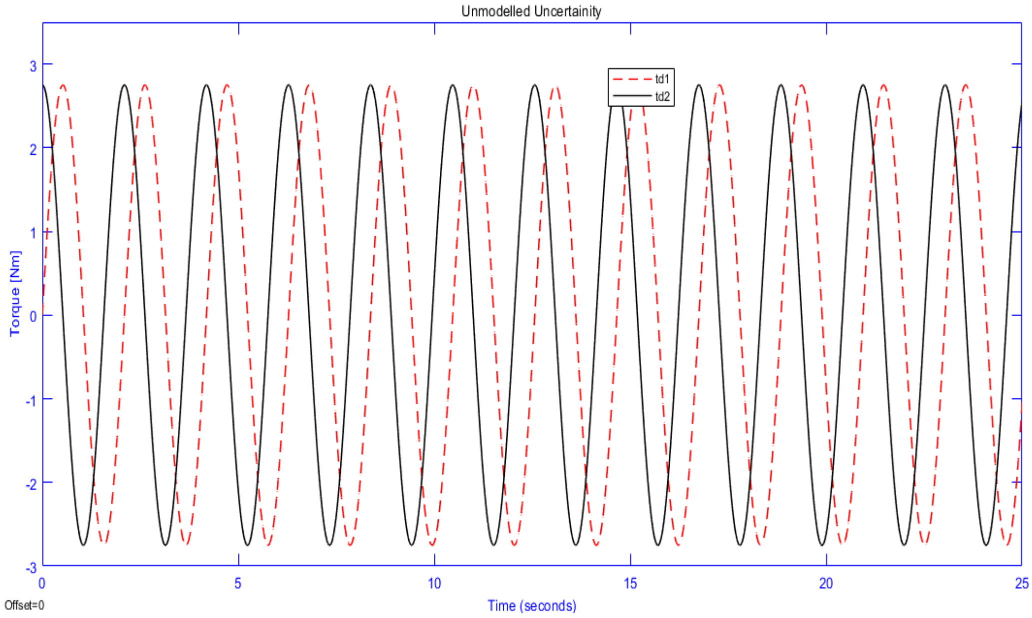

Figure 5.9: Mismatching model uncertainity disturbance.

Discussion: As seen from Figure 5.9, mismatching model uncertainity disturbance is subjected to the controller with magnitude of $t_{d1} = 2.75 * \sin(3 * t)$ and $t_{d2} = 2.75 * \cos(3 * t)$ for right and left side motor respectively.

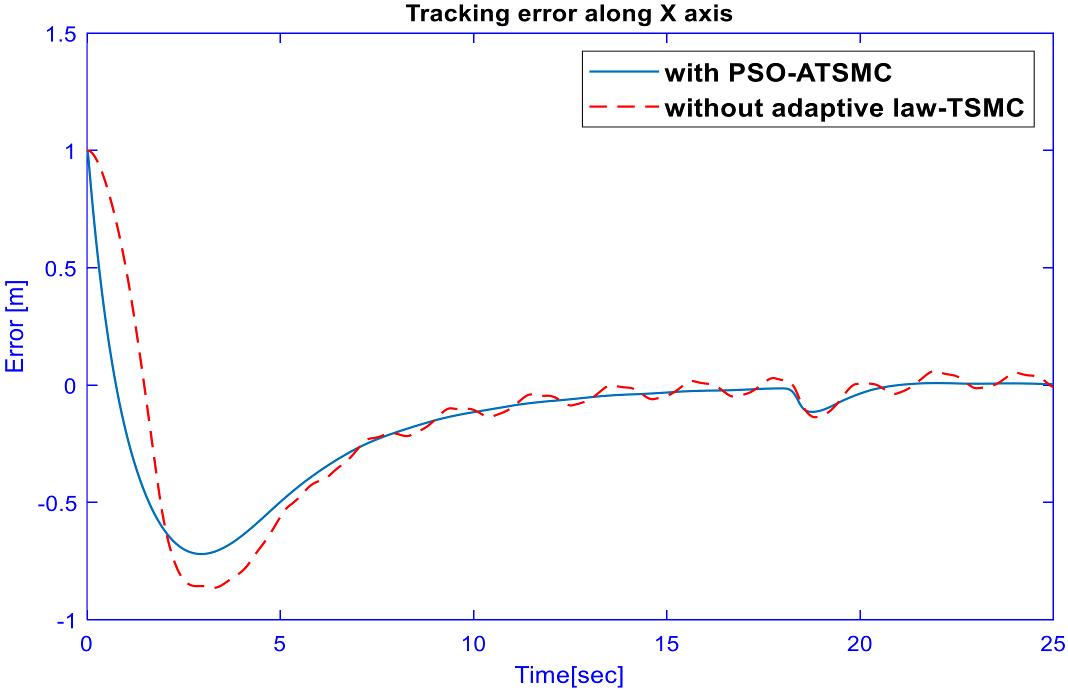

Figure 5.10: Tracking error along X axis.

Discussion: the performance of the inner loop and outer loop controller well indicated in the above Figures 5.10-5.12, which shows the robustness of the proposed controller under disturbance.

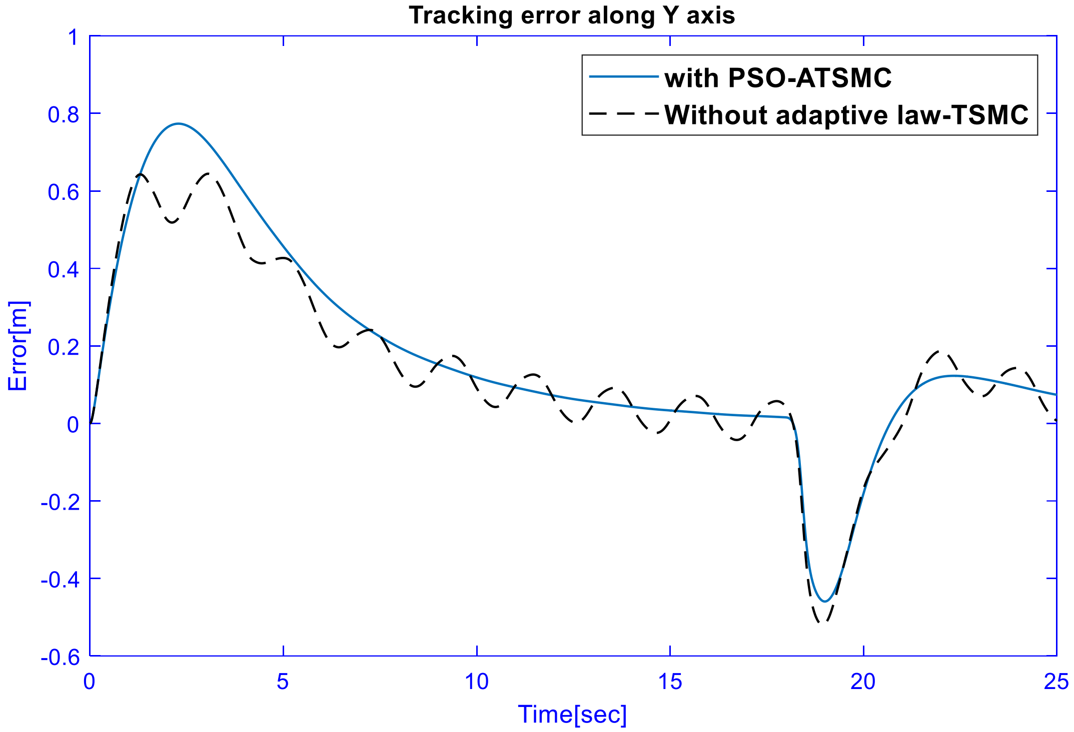

Figure 5.11: Tracking error along Y axis.

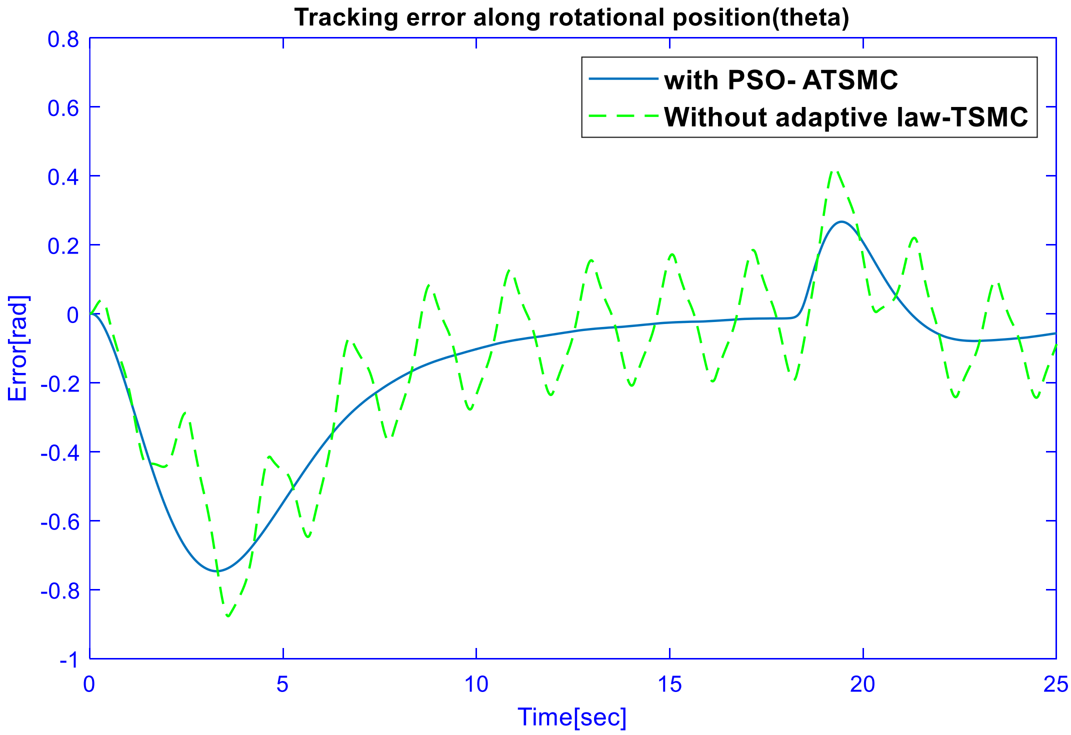

Figure 5.12: Tracking error along rotational position (theta).

Discussion: from the result of figure 5.13 and 5.14, the tracking of mobile robot along both X and Y axis (translational motion) using the PSO-adaptive TSMC is seen with respect to the reference trajectory. Similarly, the rotational position along XY plane with respect to reference trajectory is indicated in the figure 5.15 below.

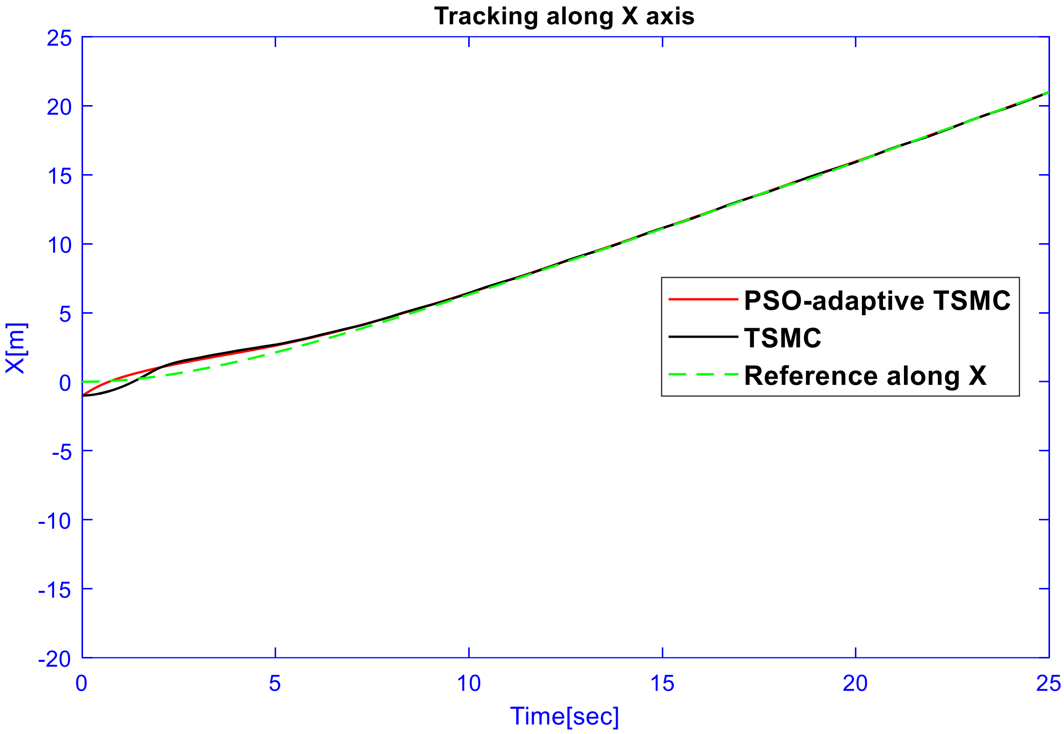

Figure 5.13: Tracking along X axis.

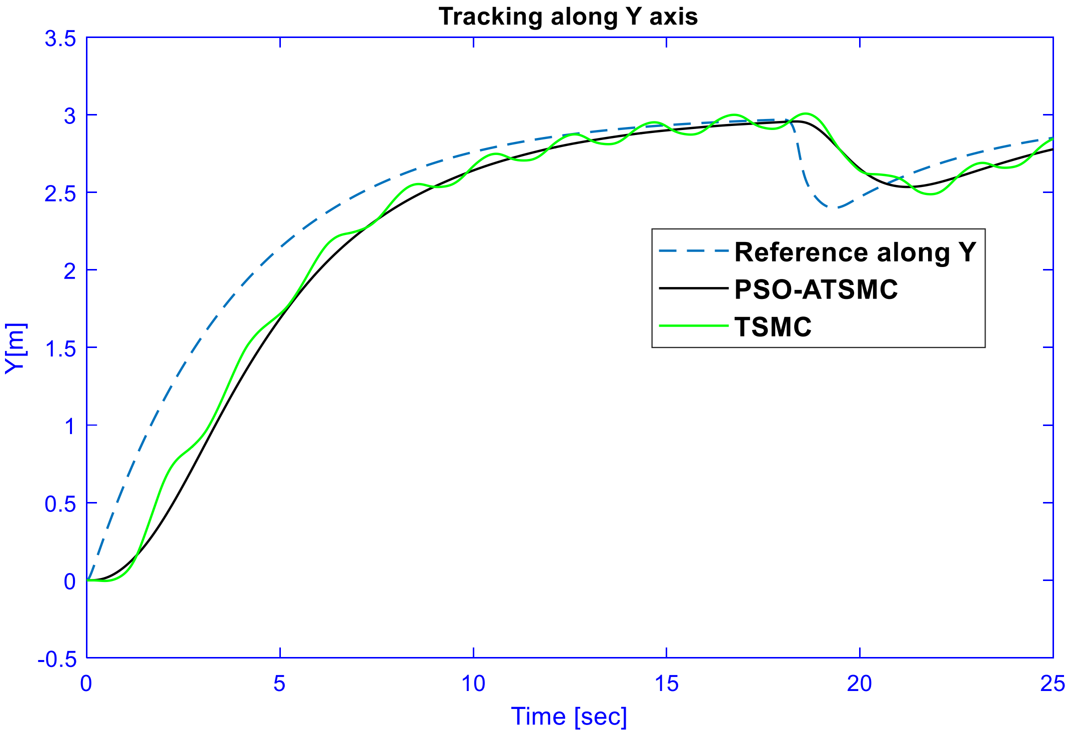

Figure 5.14: Tracking along Y axis.

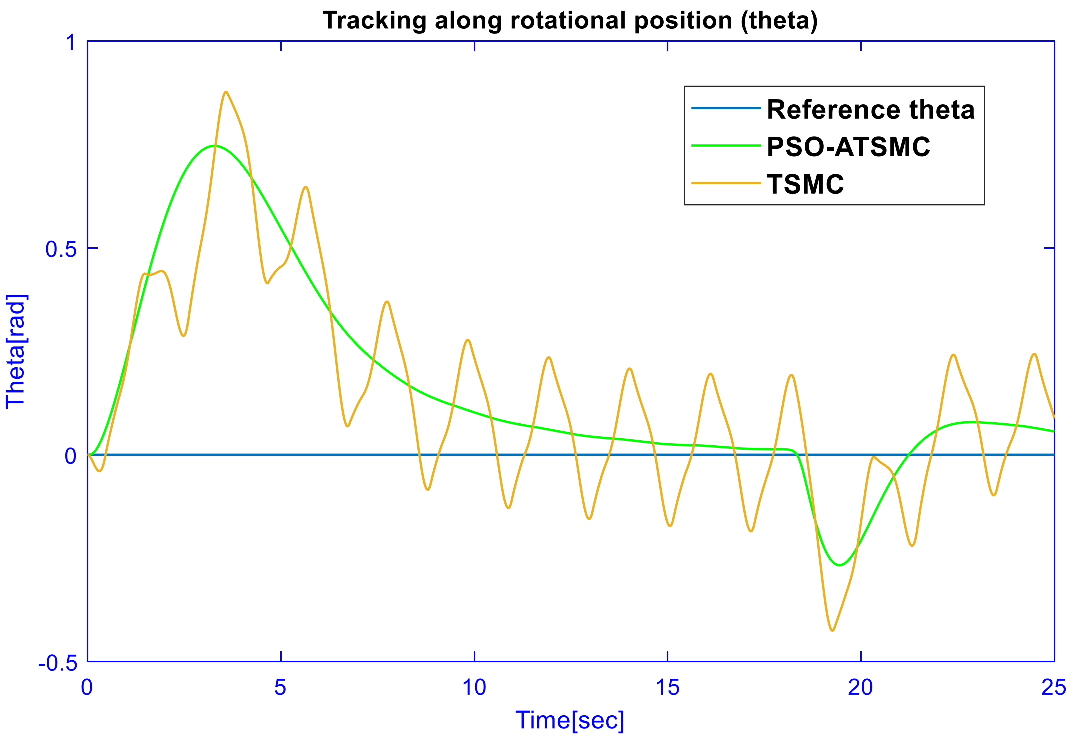

Figure 5.15: Tracking along rotational position (theta).

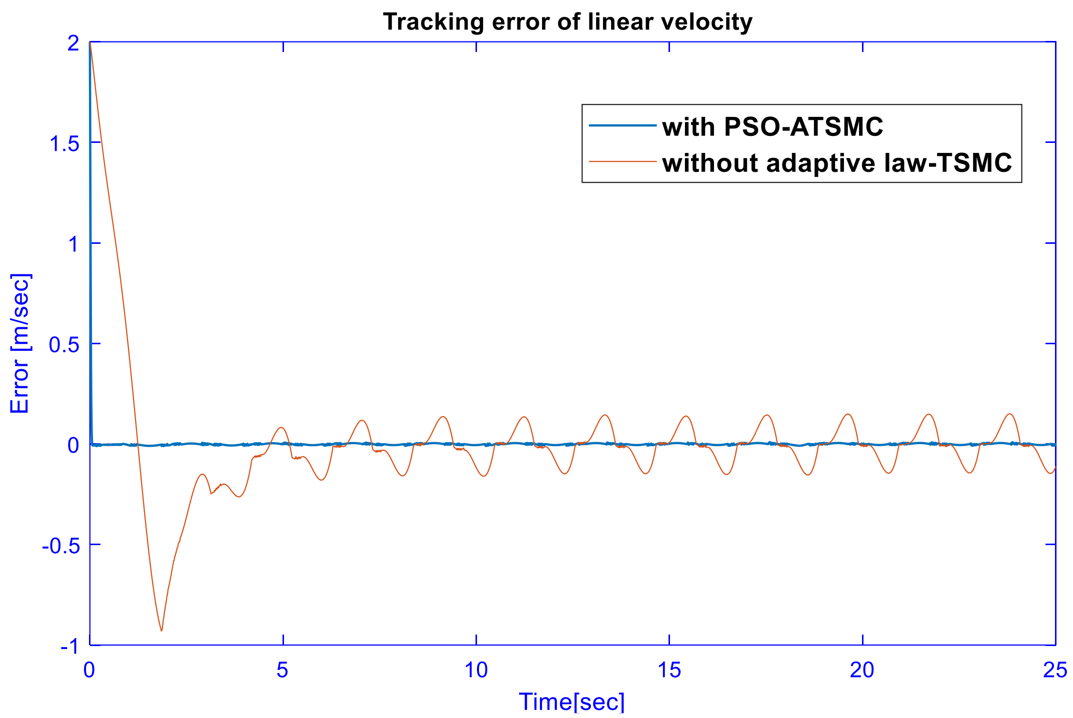

Figure 5.16: Error of linear velocity.

Discussion: performance of inner loop adaptive TSMC indicated very well in figure 5.16 and 5.17 below.

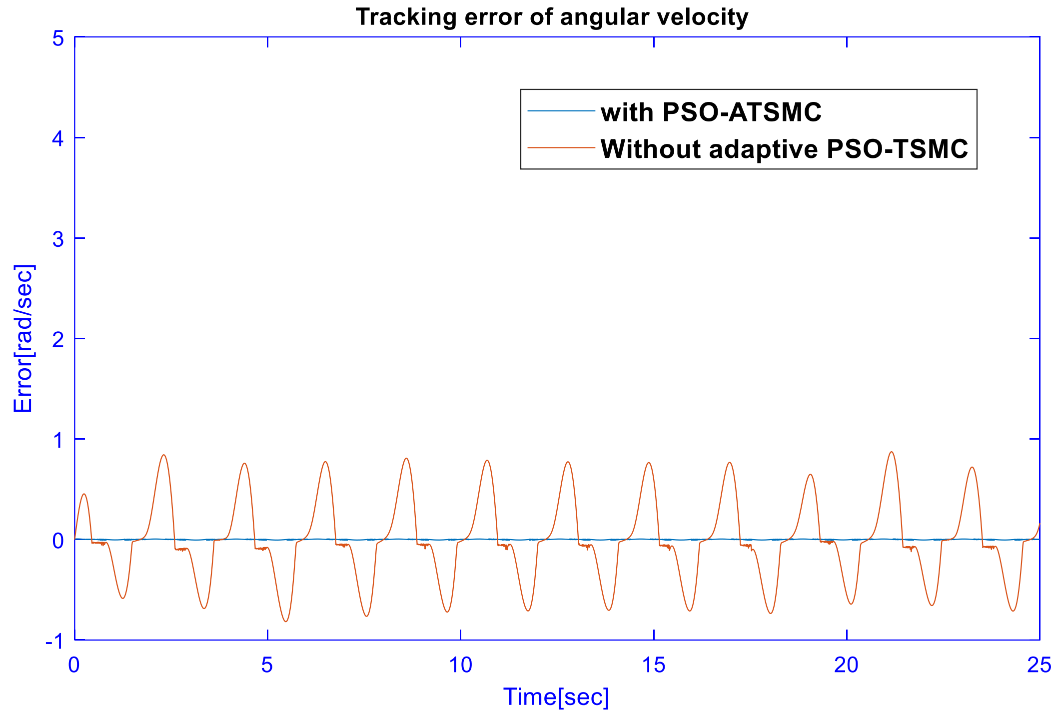

Figure 5.17: Error of angular velocity.

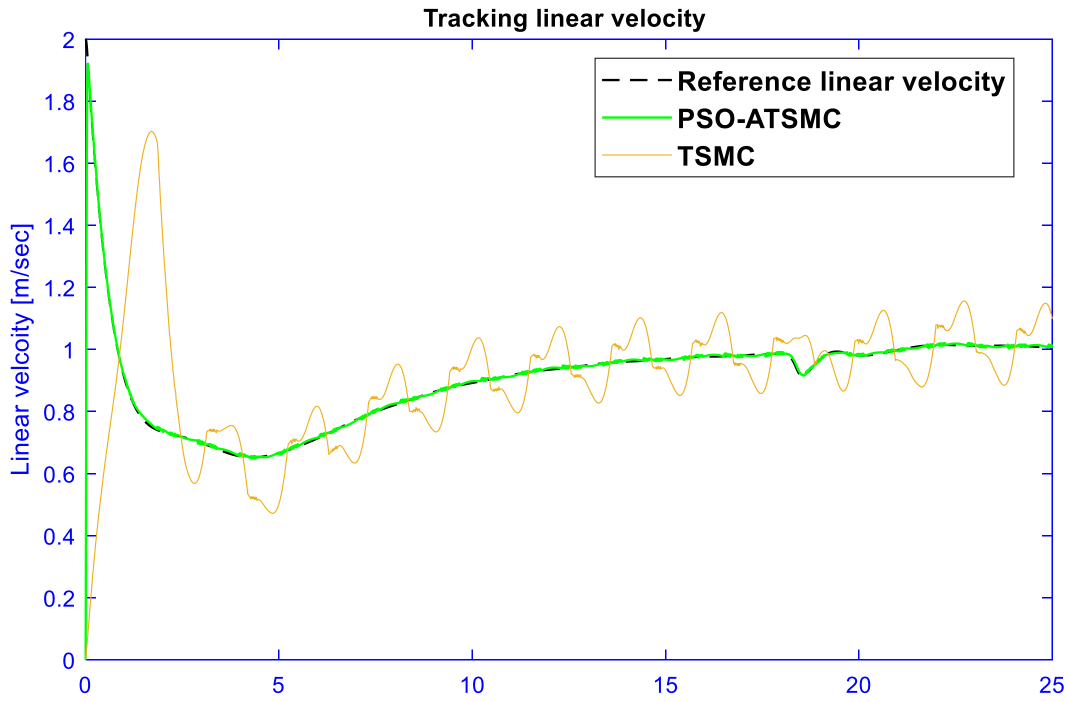

Figure 5.18: Tracking desired linear velocity.

Discussion: moreover, tracking performance of the inner controller is showed from figure 5.18 and 5.19 very well against reference trajectory.

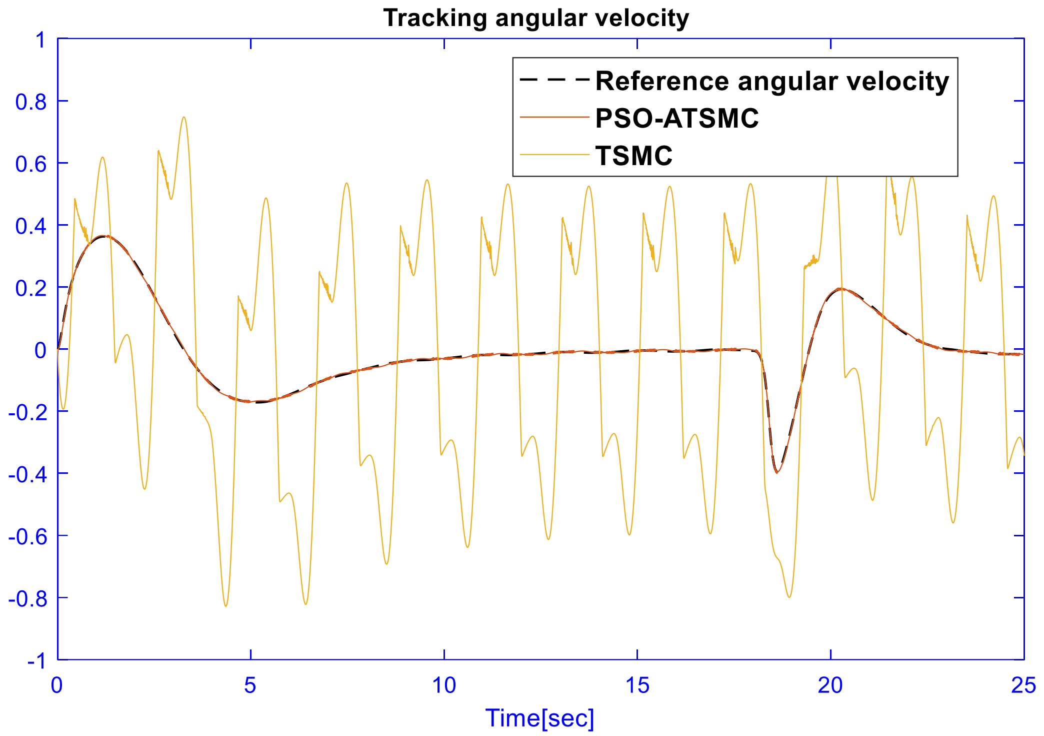

Figure 5.19: Tracking desired angular velocity.

Discussion: the magnitude control signal required the motion control system shown in the figure 5.20 and 5.21 below for both right and left wheel motors.

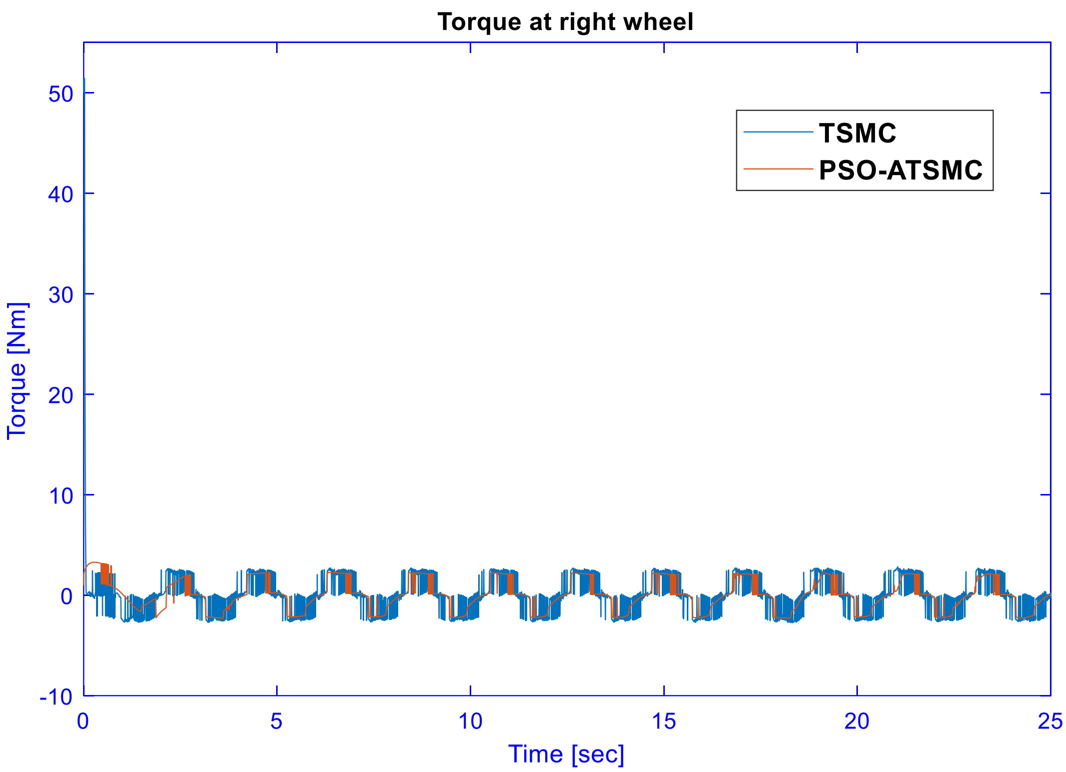

Figure 5.20: Torque at right motor.

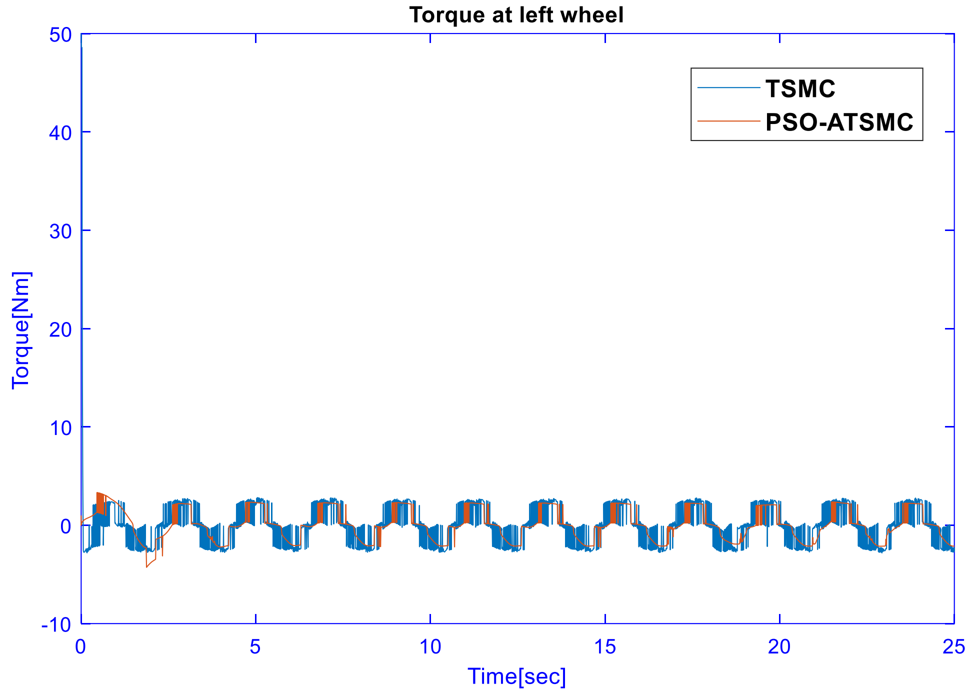

Figure 5.21: Torque at left motor.

Discussion: The XY plane trajectory under three obstacle and random disturbance is shown in Figure 5.22 below. In this case, three obstacles are placed at (20,3), (50,3) and (80,3) in order to test the controller performance against this obstacle. However, potential field function was generated appropriate reference trajectory and the controller reacts according in order to react to this time varying reference signal under static obstacles.

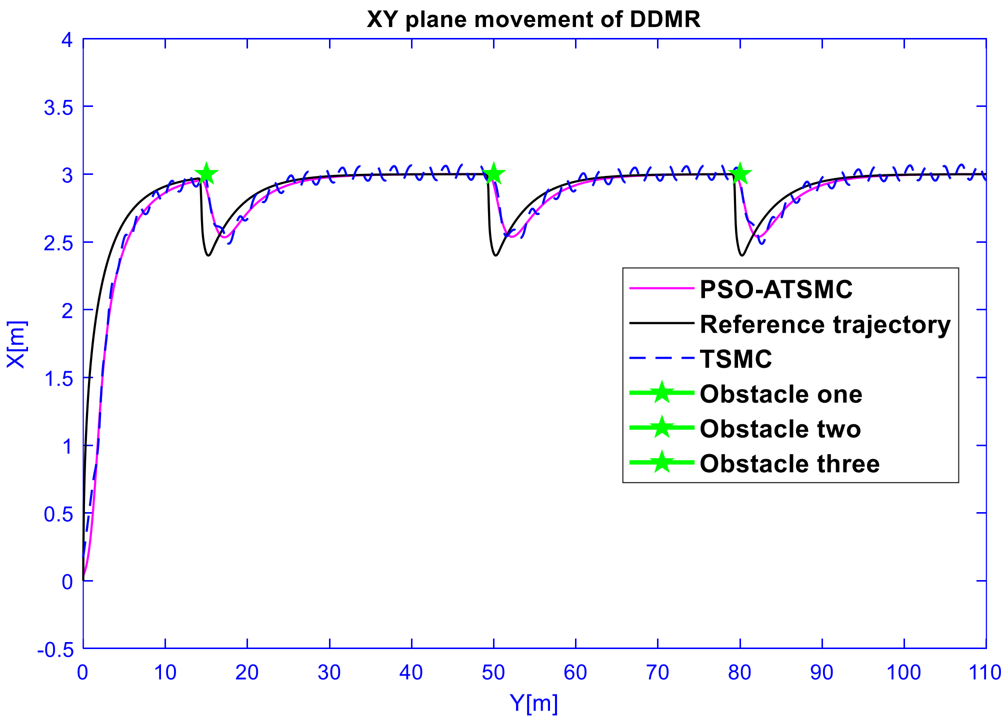

Figure 5.22: Trajectory tracking.

Discussion: the performance of the inner loop and outer loop controller well indicated in above Figure 5.22, which shows the robustness of the proposed controller under random Gaussian disturbance.

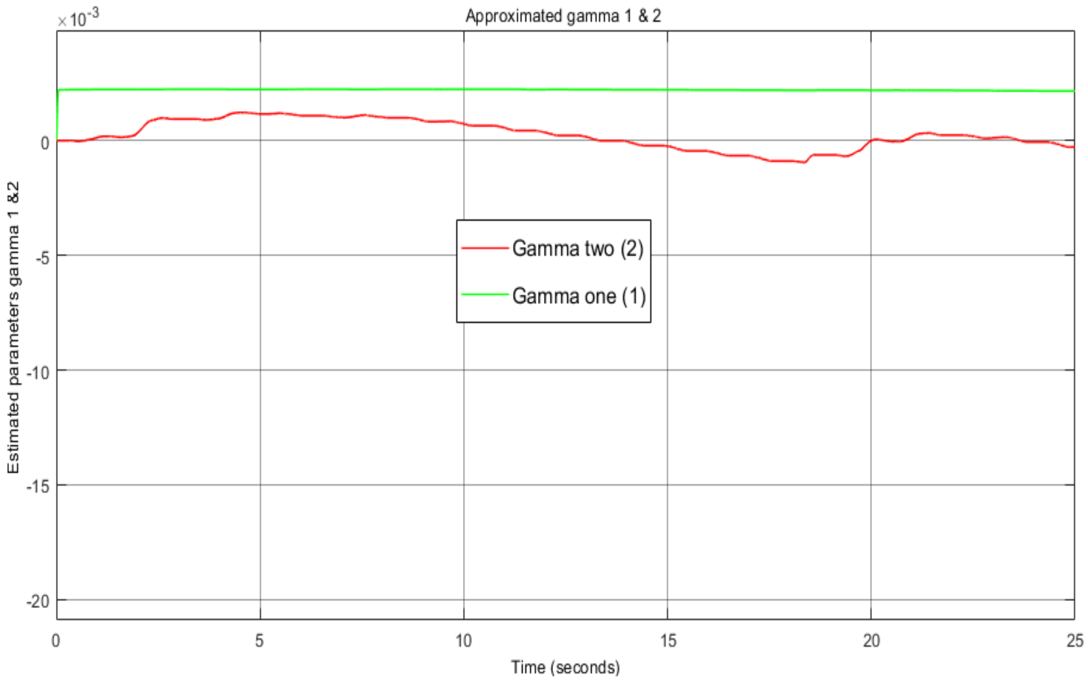

Figure 5.23: Estimated parameter of model information using adaptive law.

Discussion: from the result of figure 5.23, shows estimated uncertain parameters of mobile robot using adaptive law implemented.

Table 5. 6: Performance Metrics comparison.

Performance Metric	PSO-ATSMC Tracking			TSMC Tracking		
	Along X Axis	Along Y Axis	Along Theta	Along X Axis	Along Y Axis	Along Theta
Rise Time(sec)	1.845	2.55	3.12	2.065	3.62	4.711
Settling Time(sec)	3.157	4.209	4.21	3.638	5.11	6.337
Overshoot %	2%	8%	6%	3%	9%	7%

Discussion: Table 5. 6 demonstrate that a PSO-ATSMC significantly reduces the rise time, settling time, and overshoot when compared to TSMC.

CHAPTER SIX

6. CONCLUSION AND RECOMMENDATIONS

6.1. Conclusion

This thesis presents an advanced control strategy for a differential drive mobile robot that combines optimal adaptive terminal sliding mode control (ATSMC) with finite-time integral sliding mode control (FSMC) and gradient descent-based obstacle avoidance. The proposed control system effectively addresses the challenges of nonlinear dynamics, parameter uncertainties, and external disturbances, demonstrating significant improvements in trajectory tracking and robustness. The control architecture includes two distinct control laws: an outer loop kinematic controller for posture and angular error convergence, and an inner loop FSMC controller for precise velocity control. Parameter optimization through particle swarm optimization (PSO) has enhanced performance metrics, including trajectory tracking accuracy, velocity tracking precision, and chattering suppression. The comparative analysis of various control methods reveals that the PSO-ATSMC approach significantly outperforms traditional terminal sliding mode control (TSMC) techniques. Specifically, the PSO-ATSMC (ISE) method exhibits superior performance with minimal errors of 2.139 and 2.247 along the X and Y axes, respectively, and the smallest error of 2.101 along the θ axis. In contrast, the TSMC (ITAE) method yields larger errors of 28.27 and 42.95 along the X and Y axes, respectively, and 48.87 along the θ axis.

Additionally, the PSO-ATSMC method demonstrates improved time-domain characteristics, including reduced rise time, settling time, and overshoot, compared to the TSMC without the adaptive law. The Lyapunov-based stability analysis confirms the robustness and effectiveness of the proposed controller in maintaining desired performance despite random external disturbances and mismatched parameters. In generally, the proposed PSO-ATSMC controller offers a robust and efficient solution for the speed control of differential drive mobile robots, showcasing superior trajectory tracking performance and resilience against disturbances and parameter uncertainties. The results underscore the effectiveness of integrating adaptive control laws with sliding mode techniques to enhance control system performance in practical robotic applications.

6.2. Recommendations

The following suggestions are recommended for future work:

- Modelling of mobile robot with slip: Incorporate the effect of slip in the dynamic model of the mobile robot to enhance the accuracy of the model and control performance.
- Further design and evaluation in application areas: Extend the research to specific application areas such as welding tasks, painting robots, plantation robots, inspection robots, etc. Assess the performance of the proposed control system in real-world scenarios and evaluate its effectiveness in practical applications.
- Advanced nonlinear control system for outer loop control: Explore advanced nonlinear control techniques to enhance the outer loop control system. Investigate robust control methods, adaptive control strategies, or intelligent control approaches to improve the trajectory tracking and overall performance of the mobile robot.
- Navigation, collision avoidance, and localization using advance control mechanism like PSO, genetic algorithm.
- Implementation on hardware using digital control system: Implement the designed controller on hardware by utilizing a digital control system on a microcontroller platform. This would involve translating the controller algorithms into code and interfacing with the robot's actuators and sensors. Hardware implementation allows for real-time testing and evaluation of the control system's performance in practical scenarios.

These future directions would further advance the understanding and application of mobile robot control systems and contribute to the development of more efficient and robust robotic system

.

Reference

Abadi, A., Mekki, H., Brahim, A. B. H., Amraoui, A. E., & Ramdani, N. (2017). Optimal trajectory generation and flatness tracking control for a mobile robot. 18th International Conference on Sciences and Techniques of Automatic Control and Computer Engineering (STA). https://doi:10.1109/sta.2017.8314880

Al-Dujaili, A. Q., Falah, A., Humaidi, A. J., Pereira, D. A., & Ibraheem, I. K. (2020). Optimal super-twisting sliding mode control design of robot manipulator: Design and comparison study. *International Journal of Advanced Robotic Systems*, *17*(6), 172988142098152. https://doi.org/10.1177/1729881420981524

BeloboMevo, Benoit & Saad, Mohamad & Fareh, Raouf. (2018). Adaptive Sliding Mode Control of Wheeled Mobile Robot with Nonlinear Model and Uncertainties. 1-5. 10.1109/CCECE.2018.8447570.

D. V. P. Ankit Sharma, "Control of Mobile Robot for Trajectory Tracking by Sliding Mode Control Technique," in International Conference on Electrical, Electronics, and Optimization Techniques (ICEEOT) - 2016, Greater noida, India, 2016. (A. Sharma & Panwar, 2016)

De Luca, A., Oriolo, G., & Vendittelli, M. (2001). Control of Wheeled Mobile Robots: an experimental overview. In *Lecture notes in control and information sciences* (pp. 181–226). https://doi.org/10.1007/3-540-45000-9_8

Doria-Cerezo, A., Biel, D., Olm, J. M., & Repecho, V. (2019). Sliding mode control of a differential-drive mobile robot following a path Proceedings of the 18th European Control Conference (ECC): Naples, Italy: June 25-28, 2019". Institute of Electrical and Electronics Engineers (IEEE), p. 4061-4066. https://doi.org/10.23919/ecc.2019.8796166

E. Papadopoulos and M. Misailidis, “On differential drive robot odometry with application to path planning,” 2007 European Control Conference, ECC 2007, 03 2015.

F. S. a. A. H. Davaie-Markazi, "A new continuous approximation of sign function for sliding mode control," in International Conference on Robotics and Mechantronics (ICRoM 2018), Tehran. Iran., 2018. (Shokouhi & Markazi, 2018)

Fabregas, E., Farias, G., Aranda-Escolastico, E., Garcia, G., Chaos, D., Dormido-Canto, S., & Bencomo, S. D. (2020). Simulation and experimental results of a new control strategy for point stabilization of nonholonomic mobile robots. *IEEE Transactions on Industrial Electronics*, *67*(8), 6679–6687. https://doi.org/10.1109/tie.2019.2935976

Filippo Arbinolo.(2020). Modelling and Control of a Skid-Steering Mobile Robot for Indoor Trajectory Tracking Applications. Politecnico di Torino, Corso di laurea magistrale in Ingegneria Aerospaziale, 2020.

Guo, Y., Yu, L., & Xu, J. (2019). Robust Finite-Time Trajectory Tracking Control of Wheeled Mobile Robots with Parametric Uncertainties and Disturbances. *Journal of Systems Science and Complexity*, *32*(5), 1358–1374. https://doi.org/10.1007/s11424-019-7235-z

Hatab, R. D. a. A. (2013). Dynamic Modelling of Differential-Drive Mobile Robots using Lagrange and Newton-Euler Methodologies: A Unified Framework. *Advances in Robotics & Automation*, *02*(02). https://doi.org/10.4172/2168-9695.1000107

Hua Cen, Bhupesh Kumar Singh. (2021). Nonholonomic Wheeled Mobile Robot Trajectory Tracking Control Based on Improved Sliding Mode Variable Structure. Hindawi Wireless Communications and Mobile Computing Volume 2021, Article ID 2974839, https://doi.org/10.1155/2021/2974839

Ilyas, M., Ali, M. E., Rehman, N., & Abbasi, A. R. (2013). Design, Development & Evaluation of a Prototype Tracked Mobile Robot for Difficult Terrain. *Sir Syed University Research Journal of Engineering & Technology*, *3*(1), 7. https://doi.org/10.33317/ssurj.61 fig 2.3

Kanayama, Y., Kimura, Y., Miyazaki, F., & Noguchi, T. (1990). A stable tracking control method for an autonomous mobile robot. *Proceedings., IEEE International Conference on Robotics and Automation*, 384-389 vol.1. (Kanayama et al., 1990)

Kanjanawaniskul, K. (2017). Motion Control of a Wheeled Mobile Robot Using Model Predictive Control: A Survey. Asia-Pacific Journal of Science and Technology, *17*, 811-837.

Keighobadi, J., Sadeghi, M. S., & Fazeli, K. A. (2011). Dynamic sliding Mode controller for trajectory tracking of nonholonomic mobile robots. IFAC Proceedings Volumes, 44(1), 962–967. https://doi.org/10.3182/20110828-6-it-1002.03048

Klancar, G., Zdesar, A., Blazic, S., & Skrjanc, I. (2017). *Wheeled Mobile Robotics: From Fundamentals Towards Autonomous Systems*. Butterworth-Heinemann.

L. Jinkun et W. Xinhua, "Advanced sliding mode control for mechanical systems: design, analysis and MATLAB simulation," ed: Tsinghua University Press, Beijing CrossRef Google Scholar, 2011. (J.Liu et al.,2011)

Mevo, B. B., Saad, M. R., & Fareh, R. (2018). Adaptive sliding mode control of wheeled mobile robot with nonlinear model and uncertainties. . https://doi.org/10.1109/ccece.2018.8447570

Pang, H., Liu, M., Hu, C., & Zhang, F. (2022). Adaptive sliding mode attitude control of two-wheel mobile robot with an integrated learning-based RBFNN approach. *Neural Computing and Applications*, *34*(17), 14959–14969. https://doi.org/10.1007/s00521-022-07304-3

R. Mathew and S. S. Hiremath (. 2019), ‘‘Development of waypoint tracking controller for differential drive mobile robot,’’ in *Proc. 6th Int. Conf. Control, Decis. Inf. Technol. (CoDIT)*, Paris, France, Apr. 2019, pp. 1121–1126

Rahul Sharma K. Daniel Honc & František D. (2017).Trajectory Tracking of Differential Drive Mobile Robot by Model Predictive Control. University of Pardubice Faculty of Electrical Engineering and Informatics. http://dx.doi.org/10.1007/978-3-319-21206-7_8

Rahul, S. K., Honc, D., & Dušek, F. (2016). Predictive control of differential drive mobile robot considering dynamics and kinematics. *Proceedings - 30th European Conference on Modelling and Simulation, ECMS 2016*, 354–360. https://doi.org/10.7148/2016-0354

S. K. Malu and J. Majumdar, “Kinematics, localization and control of differential drive mobile robot,” Global Journals of Research in Engineering, vol. 14, no. H1, pp. 1–7, 2014.

Sharma, K. R., Dusek, F., & Honc, D. (2017). Comparitive study of predictive controllers for trajectory tracking of non-holonomic mobile robot. 2017 21st International Conference on Process Control (PC). https://doi.org/10.1109/pc.2017.7976213

Sharma, Rahul & Honc, Daniel & Dušek, František. (2016). Predictive Control Of Differential Drive Mobile Robot Considering Dynamics And Kinematics. DOI:10.7148/2016-0354

Singh, R., Singh, G., & Kumar, V. (2020). Control of closed-loop differential drive mobile robot using forward and reverse Kinematics. *2020 Third International Conference on*

Smart Systems and Inventive Technology (ICSSIT). https://doi.org/10.1109/icssit48917.2020.9214176

Tagliavini, L., Colucci, G., Botta, A., Cavallone, P., Baglieri, L., & Quaglia, G. (2022). Wheeled Mobile robots: state of the art overview and kinematic comparison among three omnidirectional locomotion strategies. *Journal of Intelligent & Robotic Systems*, *106*(3). https://doi.org/10.1007/s10846-022-01745-7

Torres, E.O., Konduri, S., & Pagilla, P.R. (2014). Study of wheel slip and traction forces in differential drive robots and slip avoidance control strategy. *2014 American Control Conference*, 3231-3236. 10.1109/ACC.2014.6859308. figure 2.2

Xiong, X., Reher, J., & Ames, A. D. (2021). Global Position Control on Underactuated Bipedal Robots: Step-to-step Dynamics Approximation for Step Planning. *icra*. https://doi.org/10.1109/icra48506.2021.9561961 fig 2.4

Xu, D., Liu, Q., Yan, W., & Yang, W. (2019). Adaptive terminal sliding mode control for hybrid energy storage systems of fuel cell, battery and supercapacitor. *IEEE Access*, *7*, 29295–29303. https://doi.org/10.1109/access.2019.2897015 (Xu et al., 2019)

Y. Koubaa, M. Boukattaya et T. Dammak, "Adaptive sliding-mode dynamic control for path tracking of nonholonomic wheeled mobile robot," J Autom Syst Eng, vol. 9, pp. 119-131, 2015. (Y. Koubaa et al., 2015)

Y. Shi and R. Eberhart, “A modified particle swarm optimizer,” Proceedings. IEEE World Congr. Comput. Intell. (Cat. No.98TH8360), pp. 69–73, 1998. https://doi.org/10.1109/icec.1998.699146 (Shi & Eberhart, 1998)

Yang, Y., Yan, X., Sirlantzis, K., & Howells, G. (2019). Application of Sliding Mode Trajectory Tracking Control Design for Two-Wheeled Mobile Robots. NASA/ESA Conference. https://doi.org/10.1109/ahs.2019.00012

Zhao, J.; Han, T.; Wang, S.;Liu, C.; Fang, J.; Liu, S. Design and Research of All-Terrain Wheel-Legged Robot. *Sensors* 2021, *21*, 5367. https://doi.org/10.3390/s21165367.

Appendix A

Code for potential field functions

```
function [ux,uy] = fcn(x1,x2,y1,y2,t)
%model paramters
% int x1_rec;
% int y1_rec;
% x1=0;x2=0;
% y1=0;y2=0;
alpha=4; beta=16;
obsx=15;obsy=3;
obsx1=50;obsy1=3;
obsx2=80;obsy2=3;
d=0.5;
cx=t;
cy=3;
rho=0.5*(x1-obsx)^2+(y1-obsy)^2;
rhopx=x1-obsx;
rhopy=x2-obsy;
dvx=d*(rho-d)*rhopx/((rho)^3);
dvy=d*(rho-d)*rhopy/((rho)^3);
if rho<=d;dv1=dvx; dv2=dvy;
else
dv1=0; dv2=0;
end
rho=0.5*(x1-obsx1)^2+(y1-obsy1)^2;
rhopx=x1-obsx1;
rhopy=x2-obsy1;
dvx=d*(rho-d)*rhopx/((rho)^3);
dvy=d*(rho-d)*rhopy/((rho)^3);
if rho<=d;dv11=dvx; dv22=dvy;
else
dv11=0; dv22=0;
end
rho=0.5*(x1-obsx2)^2+(y1-obsy2)^2;
rhopx=x1-obsx2;
rhopy=x2-obsy2;
dvx=d*(rho-d)*rhopx/((rho)^3);
dvy=d*(rho-d)*rhopy/((rho)^3);
if rho<=d;dv13=dvx; dv23=dvy;
```

```
else
dv13=0; dv23=0;
end
ux=-alpha*(x1-cx)-beta*x2-dv1-dv11-dv13;
uy=-alpha*(y1-cy)-beta*y2-dv2-dv22-dv23;
```

Code for adaptive particle swarm optimization:

```
clc; clear all; close all;
%model paramters
tf=10;
% pso constant parameters
c=2;particles=20;iteration=30;var=6;var1=2;
%search space
a=1;
b=2;
a1=1;
b1=10;
wmax=0.9;
wmin=0.1;
%initialization position and velocity of each decision variables
for m=1:particles
for n=1:var
v(m,n)=0;
x(m,n)=a+rand*(b-a);
xp(m,n)=x(m,n);
end
A=x(m,1);
y1=x(m,2);
a2=x(m,3);
y2=x(m,4);
B=x(m,5);
b2=x(m,6);
for n=1:var1
v1(m,n)=0;
x1(m,n)=a1+rand*(b1-a1);
xp1(m,n)=x1(m,n);
end
k=x1(m,1);
k1=x1(m,2);
%run simulink
```

```
sim('Final')
ISE(m)=sum(se_sim+se_sim1+se_sim2);
end
% best global value
[Best_perfomance,location]=min(ISE);
fg=Best_perfomance;
xg(1)=x(location,1);
xg(2)=x(location,2);
xg(3)=x(location,3);
xg(4)=x(location,4);
xg1(1)=x1(location,1);
xg1(2)=x1(location,2);
xg(5)=x(location,5);
xg(6)=x(location,6);
% xg1(1)=x1(location,1);
% xg1(2)=x1(location,2);
% xg1(3)=x1(location,3);
%main loop
for i=1:iteration
w=wmax-((wmax-wmin)/iteration)*i;
for m=1:particles
disp(['iteration' num2str(i) ': best cost=' num2str(fg)]);
for n=1:var
v(m,n)=w*v(m,n)+c*rand*(xp(m,n)-x(m,n))+c*rand*(xg(n)-x(m,n));
x(m,n)=x(m,n)+v(m,n);
end
for n=1:var
if x(m,n)<a;x(m,n)=a;end
if x(m,n)>b;x(m,n)=b; end
end
A=x(m,1);
y1=x(m,2);
a2=x(m,3);
y2=x(m,4);
B=x(m,5);
b2=x(m,6);
for n=1:var1
v1(m,n)=w*v1(m,n)+c*rand*(xp1(m,n)-x1(m,n))+c*rand*(xg1(n)-x1(m,n));
x1(m,n)=x1(m,n)+v1(m,n);
end
for n=1:var1
```

```
if x1(m,n)<a1;x1(m,n)=a1;end
if x1(m,n)>b1;x1(m,n)=b1; end
end
k=x1(m,1);
k1=x1(m,2);
%run simulink
sim('Final')
% new personal best value
ISE1(m)=sum(se_sim+se_sim1+se_sim2);
if ISE1(m)<ISE(m)
ISE(m)=ISE1(m);
xp(m,1)=x(m,1);
xp(m,2)=x(m,2);
xp(m,3)=x(m,3);
xp(m,4)=x(m,4);
xp1(m,1)=x1(m,1);
xp1(m,2)=x1(m,2);
xp(m,5)=x(m,5);
xp(m,6)=x(m,6);
%         xp1(m,1)=x1(m,1);
%         xp1(m,2)=x1(m,2);
%         xp1(m,3)=x1(m,3);
end
end
%global best value
[B_fg,location]=min(ISE);
if B_fg<fg
fg=B_fg;
xg(1)=xp(location,1);
xg(2)=xp(location,2);
xg(3)=xp(location,3);
xg(4)=xp(location,4);
xg1(1)=xp1(location,1);
xg1(2)=xp1(location,2);
xg(5)=xp(location,5);
xg(6)=xp(location,6);
% xg1(1)=xp1(location,1);
% xg1(2)=xp1(location,2);
% xg1(3)=xp1(location,3);
end
end
```

```
A=xg(1);
y1=xg(2);
a2=xg(3);
y2=xg(4);
B=xg(5);
k=xg1(1);
b2=xg(6);
k1=xg1(2);
%    kx=xg1(m,1);
%    ky=xg1(m,2);
%    kz=xg1(m,3);
```

Code for projection of control signal:

```
function y = fcn(u,u1)
mw=0.5;
mc=17;
ic=0.537;
iw=0.0023;
im=0.0011;
r=0.095;
l=0.24;
d=0.05;
m=mc+2*mw;
i=ic+mc*d^2+2*mw*l^2+2*im;
a11=m+((2*iw)/(r^2));
a12=i+((2*(l^2)*iw)/(r^2));
% th_max=a11*r;
th_max=37.51;
th_min=17.51;
if u1>=th_max&&u>0
y=0;
elseif u1<=th_min&&u<0
y=0;
else
y=u;
end
```

Simulink block diagram of ATSMC:

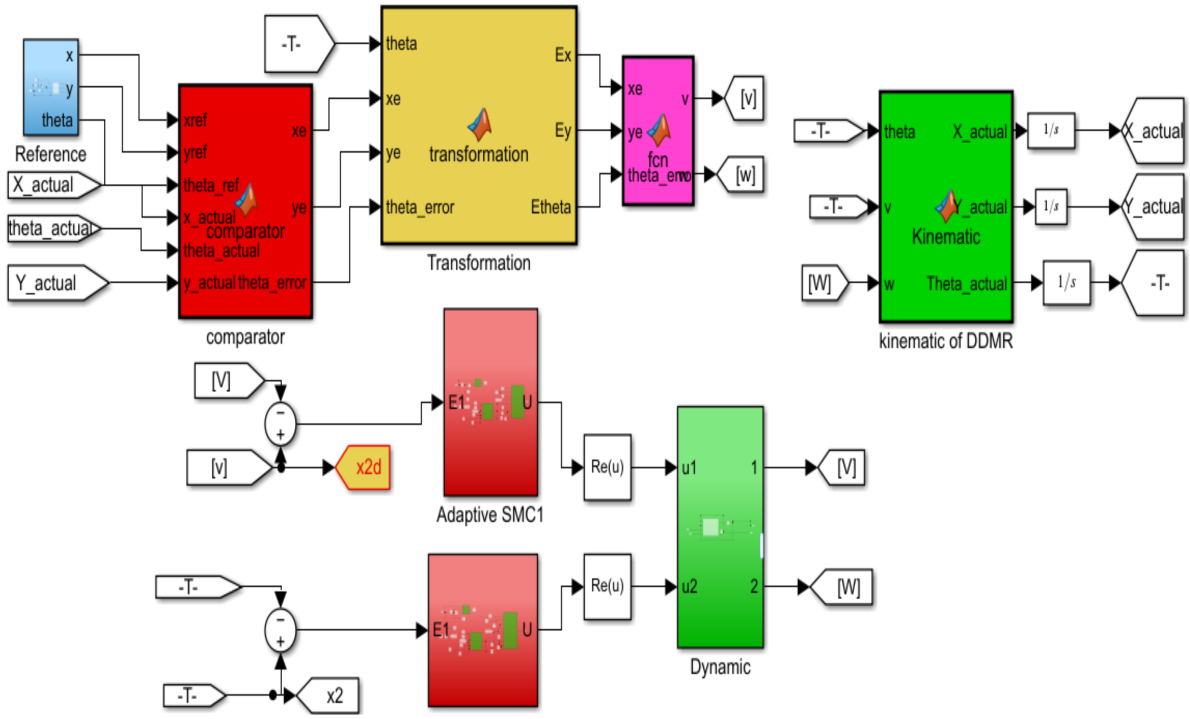

Document ID: 66eda38dd727a93bf5e931d9
Document Name: final draft for becky corrected
Document Pages: 82

Document Status: Completed
Document Completion Date: September 20, 2024, 16:34 UTC

Signer: almaz (almaztekle24@gmail.com)

Signer	Signature	Timestamps
almaz almaztekle24@gmail.com Using IP: 196.190.52.209 IP Location: Ethiopia, Addis Ababa Authentication method: Email		Viewed: September 20, 2024, 16:34 UTC Signed: September 20, 2024, 16:34 UTC